Evolution, 2026, **0(0)**, 1–18
https://doi.org/10.1093/evolut/qpag083
Advance access publication 6 May 2026
Original Article

History of divergence and gene flow shaping geographic variation in Andean warblers (*Myioborus*)

Laura N. Céspedes Arias[1,2], Andrés M. Cuervo[3], Carlos Daniel Cadena[4], Elisa Bonaccorso[5], Christopher Witt[6], Irby Lovette[7,8], Leonardo Campagna[7,8]

[1]Committee on Evolutionary Biology, The University of Chicago, Chicago, IL, United States
[2]Birds Division, Field Museum of Natural History, Chicago, IL, United States
[3]Instituto de Ciencias Naturales, Facultad de Ciencias, Universidad Nacional de Colombia, Bogotá, Colombia
[4]Departamento de Ciencias Biológicas, Universidad de los Andes, Bogotá, Colombia
[5]Laboratorio de Biología Evolutiva, Colegio de Ciencias Biológicas y Ambientales, Universidad San Francisco de Quito, Quito, Ecuador
[6]Museum of Southwestern Biology, University of New Mexico, Albuquerque, NM, United States
[7]Fuller Evolutionary Biology Program, Cornell Lab of Ornithology, Ithaca, NY, United States
[8]Department of Ecology and Evolutionary Biology, Cornell University, Ithaca, NY, United States

Corresponding author: Field Museum of Natural History, 1400 S. Jean Baptiste Pointe DuSable Lake Shore Drive, Chicago, IL 60605; E-mail: lncespedesarias@gmail.com

Abstract

Studying how genetic variation is structured across space, and how it relates to divergence in phenotypic traits relevant to reproductive isolation, is important for our understanding of the speciation process. We used ddRAD-seq data to examine genetic variation across the distribution of an Andean warbler species complex (*Myioborus ornatus–melanocephalus)*, which includes a known hybrid zone between two taxa with striking plumage differences. Genetic structure reflects geographic variation in head plumage, with some breaks coinciding with major topographic barriers in the Andes. We found that *M. o. chrysops* and *M. m. bairdi*, the two hybridizing taxa, were characterized by low overall genetic divergence. Based on our cline analyses of plumage and genomic hybrid indices, this hybrid zone extends for approximately 250 km, where advanced generation hybrids are likely most common. We also identified a slight difference in the geographic centers of the plumage and genetic ancestry clines, potentially suggesting asymmetric introgression of *chrysops*-like plumage traits. By studying genetic variation in a phenotypically diverse group distributed across a topographically complex area that includes a hybrid zone, we show how both geographic features and plumage traits potentially relevant to mate choice may contribute to species formation and maintenance in tropical mountains.

Keywords: phylogeography, hybrid zone, reduced representation genomic data, geographic variation, Parulidae

Introduction

Geographic variation in traits relevant to reproductive isolation is often viewed as a snapshot of the early stages of population divergence (Mayr, 1942; Price, 2008), making it a focus for understanding the process of speciation. To study this process, it is useful to evaluate how phenotypic variation in such traits is related to the underlying population genetic structure (Edwards et al., 2016; Zamudio et al., 2016). A common expectation is that phenotypic and genetic divergence are positively correlated: in the absence of strong divergent selection, extended periods of isolation are typically required for phenotypic differentiation to evolve (Nosil, 2008; Price, 2008; Winger & Bates, 2015). It follows that range disjunctions associated with topographic and ecological barriers, which restrict gene flow, are expected to be accompanied by genetic and phenotypic discontinuities (Edwards et al., 2016). However, geographic variation in phenotypic traits is not always concordant with genetic structure. This discordance may result from complex histories of selection and gene flow leading to phenotypic convergence (Márquez et al., 2020), strong selection on specific traits across steep environmental gradients (Mullen & Hoekstra, 2008) or selection on mate-choice-related traits in zones of secondary contact, leading to differential introgression (Baldassarre et al., 2014; Lim et al., 2024; Stein & Uy, 2006b). A better understanding of how species diversify across space requires studying such histories of isolation, and how these relate to divergence in traits, particularly those that might be important for mate choice and, consequently, reproductive isolation.

Patterns of plumage differentiation—thought to be important for reproductive isolation in birds (Price, 2008; Uy et al., 2018)—across allopatric populations within species are pervasive among Andean birds (Graves, 1988; Remsen, 1984). Although geographic variation in plumage and genetic structure in Andean birds is often associated with current topographic and ecological barriers (Gutiérrez-Pinto et al., 2012; Prieto-Torres et al., 2018), many of these barriers tend to be permeable and unstable over evolutionary timescales. Dispersal across such barriers could lead to introgressive hybridization connecting otherwise diverging populations (Winger, 2017). Additionally, differentiated popula-

Received August 25, 2025; revisions received March 27, 2026; accepted April 24, 2026
Associate Editor: Scott Taylor; Handling Editor: Hélène Morlon

tions may come into renewed contact as barriers change over time. In the particular case of the Andes, climatic fluctuations (Ramírez-Barahona & Eguiarte, 2013) and, potentially, volcanic activity (Sanín et al., 2024) have promoted cycles of fragmentation and reconnection of elevational vegetation belts, creating opportunities for contact among periodically isolated populations (Vuilleumier, 1969). Examining these complex histories of divergence and gene flow in geographically variable Andean taxa contributes to a more comprehensive understanding of how bird species are formed and maintained in this biodiversity hotspot (Rahbek et al., 2019; Sonne et al., 2022).

Here, we used a reduced-representation genomic data set from an Andean bird species complex of *Myioborus* warblers (Parulidae) characterized by striking geographic variation in head color patterns to gain insights into differentiation in geographically isolated populations and the processes that occur after differentiated populations come into secondary contact. This young (<1 my; Cuervo, 2013) species complex inhabits the high Andes from Bolivia to Venezuela, and is characterized by differences in head color patterns despite shallow genetic differentiation in mitochondrial DNA (Céspedes-Arias et al., 2021; Pérez-Emán, 2005). Seven plumage groups have been described as subspecies belonging to two species, *Myioborus ornatus* and *M. melanocephalus*, distributed mostly allopatrically along different sections of the Andes (Cuervo & Céspedes-Arias, 2023; Zimmer, 1949). According to this classification scheme, *M. ornatus* includes subspecies *ornatus* and *chrysops*, and *M. melanocephalus* includes subspecies *bairdi* (also known as *ruficoronatus*; but see Cuervo & Céspedes-Arias, 2023), *griseonuchus*, *malaris*, *melanocephalus*, and *bolivianus*. Recent taxonomic revisions, however, suggest that a four-species classification scheme might better capture current knowledge of genetic and plumage variation in this complex (Cuervo & Céspedes-Arias, 2023). Regardless of the species delimitation scheme, analyses based on the ND2 mitochondrial gene have revealed extensive haplotype sharing among groups with conspicuous plumage differences, potentially suggesting a history of rapid plumage evolution or repeated mitochondrial introgression (Céspedes-Arias et al., 2021).

Our previous work in regions where the ranges of *chrysops* and *bairdi* abut, on the border between Colombia and Ecuador, revealed that these two taxa hybridize widely across more than 200 km, where individuals with a variety of intermediate head color patterns occur (Céspedes-Arias et al., 2021). Although hybridization has been extensive there, the existence of a sharp plumage cline, limited to a relatively narrow zone within these taxa's broader ranges (20%−30% of the entire distribution), suggests the action of some form of selection maintaining their differentiation (Barton & Hewitt, 1985; Brelsford & Irwin, 2009; Harrison, 1986). Here, we leveraged this previous systematic collection and detailed plumage characterization of the *bairdi* × *chrysops* hybrid zone (Céspedes-Arias et al., 2021) to gain a deeper understanding of hybridization dynamics using genomic data.

The study of hybrid zones across a diversity of taxa, including birds, has played a central role in shaping our understanding of species formation and maintenance (Abbott et al., 2016; Harrison, 1990). In birds, a high proportion of detailed genomic studies of hybrid zones have focused on temperate species, providing key insights, among others, into heterogeneous patterns of genome-wide introgression, the temporal movement of hybrid zones, and the genetic architecture of phenotypic traits (Aguillon et al., 2021; Blain et al., 2025; Brelsford et al., 2017; De Zwaan et al., 2022; Taylor et al., 2014). In the tropical Americas, much of the recent genomic work on hybrid zones has focused on lowland taxa, particularly in Amazonia, highlighting the importance of river dynamics and their historical fluctuations in shaping patterns of hybridization (Cronemberger et al., 2020; Pulido-Santacruz et al., 2018; Weir et al., 2015). Despite the exceptional species richness of the tropical Andes, detailed genomic studies of hybrid zones in Andean taxa remain relatively rare. The few well-characterized Andean hybrid zones involve elevational replacements, including *Ramphocelus* tanagers (Castaño et al., 2026; Morales-Rozo et al., 2017) and *Anairetes* flycatchers (Dubay & Witt, 2014). The *Myioborus* hybrid zone offers a distinct window into the processes that follow secondary contact of latitudinal replacements without an obvious physical barrier and that occupy the same elevational band. While other hybrid zones among such taxa have been identified using phenotypic or genomic data (Graves, 1982; Muñoz-Quintana & Cuervo, 2024; Schmitt, 2022), our dense sampling across the contact zone, coupled with broad geographic sampling of related populations, provides a uniquely detailed perspective on gene flow and divergence in a complex Andean landscape.

We examined patterns of genomic variation within this warbler species complex at two different spatial scales: the entire distribution of the species complex, which corresponds to a broad latitudinal band in the Andes (~3800 km in geographic distance), and the hybrid zone between two markedly different plumage groups, as outlined above. By focusing on these two scales, we addressed questions related to multiple processes relevant to the formation and maintenance of species. First, leveraging a broad geographic-scale sampling of individuals representing all plumage forms in the complex, we asked: (1) How is genetic structure related to geographic distance, topography, and plumage variation along the Andes? At a finer spatial scale, in the hybrid zone between two plumage forms, we asked: (2.1) Does the geographic pattern of introgression mirror plumage variation across the hybrid zone? And (2.2) is there evidence for non-neutral processes such as selection against hybrids based on patterns of genomic variation? Our genome-wide data coupled with dense geographic sampling substantially improves our ability to reconstruct and understand the diversification history of these colorful montane warblers, which was previously limited to studies using only a single mitochondrial gene.

Methods

Study species and sampling

The taxonomic classification within this species complex is in flux, and its reassessment is beyond the scope of this study. For consistency, we follow the classification scheme as accepted by the Birds of the World (Clements et al., 2025): *M. ornatus* (including subspecies *ornatus* and *chrysops*) and *M. melanocephalus* (including subspecies *bairdi*, *griseonuchus*, *malaris*, *melanocephalus*, and *bolivianus*). The specific epithet *bairdi* is used here instead of *ruficoronatus*, as currently listed in Birds of the World, to reflect definitive evidence that

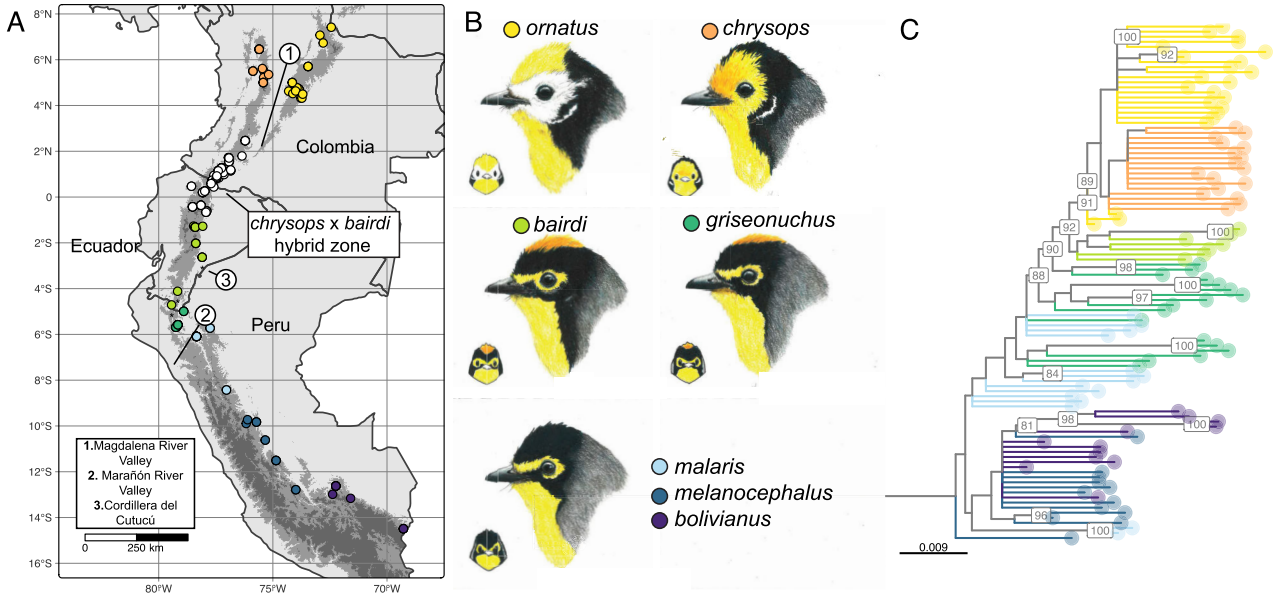

Figure 1. Sampling localities of specimens included in the study (A), which encompass all subspecies (B). The color of the dots corresponds to study taxa. The white dots correspond to areas around the *bairdi* × *chrysops* hybrid zone as identified based on plumage patterns (Céspedes-Arias et al., 2021). The subspecies *malaris*, *melanocephalus*, and *bolivianus*, which are similar in facial pattern, are here represented by one illustration. In the map, elevation is denoted by the grayscale in the background, with the elevation in which these *Myioborus* occur shown in an intermediate shade of gray. The localities marked with an asterisk correspond to those in Loja and outlying ridges in Morona–Santiago that are discussed in the main text, and numbers mark important topographic features. (C) Maximum-likelihood phylogeny estimated with our dataset of concatenated ddRAD loci, showing how overall relationships somewhat reflect geography (outgroups not shown). The terminal branches are colored by subspecies as in the map. Only bootstrap values over 70 are shown, and nodes with a support lower than 50 were collapsed into polytomies. Hybrid zone samples were not included in the analysis. Illustrations: Andrés Montes Rojas.

the type specimen of *ruficoronatus* corresponds to a hybrid and is therefore a void name (Cuervo & Céspedes-Arias, 2023; Remsen et al., 2026). Throughout this paper, we refer to subspecies (i.e., geographically circumscribed plumage groups) using their subspecific epithet.

We used tissue samples collected across the distribution of the *M. ornatus–melanocephalus* complex ($n = 227$, Figure 1.; Céspedes-Arias et al., 2021) and previously deposited in museum collections (Table S1). Samples encompassed all seven subspecies and a denser sampling in the *bairdi* × *chrysops* hybrid zone area, along the border between Colombia and Ecuador (Figure 1A). We also obtained data for eight individuals as outgroup, corresponding to three other species in *Myioborus*: *M. pictus* ($n = 3$), *M. miniatus* ($n = 3$), and *M. brunniceps* ($n = 2$), which vary in their phylogenetic and geographic proximity to the *M. ornatus–melanocephalus* complex (Lovette et al., 2010; Pérez-Emán, 2005). Additional details about subspecies distributions and plumage descriptions are available in the Supplementary Material (Text S1, also see Figure S1).

Laboratory procedures

DNA extraction and library preparation

We extracted genomic DNA from pectoral muscle ($n = 232$) and blood samples ($n = 3$) employing a modified phenol–chloroform protocol (Sambrook, 1987), using phase-lock tubes. Each DNA extraction was subsequently purified using homemade Sera-Mag Magnetic SpeedBeads for magnetic nucleic acid extraction. To obtain reduced-representation genomic data, we used double-digest restriction site-associated DNA sequencing (ddRAD) following Peterson et al. (2012) with modifications from Thrasher et al. (2018). The genomic libraries were then sequenced on a single HiSeq2500 Illumina lane (100 bp single-end) by the Genomics Core Facility of Cornell University. Further details on DNA extractions and genomic library preparation can be found in the Supplementary Material (Text S2).

Bioinformatics pipeline

Quality assessment, filtering, and demultiplexing

We assessed sequence quality using FastQC (Andrews, 2010). We used the *process_radtags* function implemented in STACKS 2.66 (Rochette et al., 2019) to demultiplex the reads and apply quality filters. Specifically, we filtered out all reads with uncalled bases, those with a Phred quality score below 20, and those that did not pass the Illumina chastity/purity filter. After demultiplexing, we checked the number of reads available per individual and only kept samples with 200,000 or more reads (Figure S2). Using this threshold, we discarded 11 individuals, mostly corresponding to the *ornatus* group and tissues collected around ten years prior to this study (range of number of reads for these individuals = 960−150,152). Despite discarding these samples, 23 high-quality samples for the *ornatus* group remained in downstream analyses. Following these exclusions, we kept a total of 242,204,894 reads corresponding to 224 individuals at this stage.

Integrated assembly

After demultiplexing, we assembled the RAD reads *de-novo* using functions implemented in STACKS 2.66 (Rochette et al., 2019), and later integrated position information for the

loci in the catalog from a reference genome (Paris et al., 2017; Rivera-Colón & Catchen, 2022). This integrated approach performs better than directly mapping reads onto a reference genome in some scenarios, for example, if the reference genome is relatively distant to the study species as is our case (Paris et al., 2017). We used the chromosome-level assembly of the *Setophaga coronata* genome (Baiz et al., 2021) as a reference, the highest quality available genome within Parulidae. The time to the most recent common ancestor between *Setophaga* and *Myioborus* is estimated between 5 and 7 mya (Barker et al., 2015).

Before assembling the reads, we conducted an optimization of the parameters *M* and *n* used by *denovo_map.pl* (Rochette et al., 2019), for three different assemblies: one including representatives from the outgroup, one that only included individuals within the *ornatus–melanocephalus* complex, and one including only samples relevant for the hybrid zone analyses (*chrysops*, individuals in the hybrid zone, *bairdi*, and *griseonuchus*, Figure 1). A detailed explanation of these optimization steps is provided in the Supplementary Material (Text S3), and the results are summarized in Table S2.

After the optimization runs, we ran *denovo_map.pl* for the entire dataset with the chosen parameter values ($n = 224$ for the full assembly, $n = 216$ for the ingroup-only assembly, and $n = 123$ for the hybrid zone assembly). We then mapped the de novo catalogs to the reference genome using *bwa* (Li & Durbin, 2009). After excluding four individuals with a mean effective coverage lower than 20x (Figure S3), 221 individuals were retained for downstream analyses. A full description of each of the integrated assembly steps and results (i.e., coverage and mapping rates) can be found in the Supplementary Material (Text S3).

SNP datasets

We obtained different SNP datasets to be used in downstream analyses using the *populations* program from STACKS 2.66 (Rochette et al., 2019). For some analyses, we further filtered SNPs using VCFtools (Danecek et al., 2011). A detailed description of how the datasets were obtained is provided in the Supplementary Material (Text S4), including our rationale for the chosen filtering parameter values. A summary of filtering parameters and resulting number of SNPs per dataset used in each analysis is shown in Table S3.

Analyses of diversification within the *ornatus–melanocephalus* complex

Phylogenetic and admixture graph inference

With the goal of inferring the overall relationships among subspecies, we employed two methods to build phylogenies and also inferred admixture graphs. For this set of analyses, we excluded all individuals from or adjacent to the hybrid zone (in white, Figure 1) and the *griseonuchus–bairdi* transition area (arrows, Figure 1) and used the assembly that includes outgroup taxa (*M. pictus*, *M. miniatus*, *M. brunniceps*). For phylogenetic approaches, we included all outgroup individuals (total $n = 110$), while for the admixture graph inference, we only included one outgroup (total $n = 105$).

RAxML-NG: We used RAxML-NG (Kozlov et al., 2019) to infer maximum-likelihood trees from concatenated ddRAD loci, including both variant and invariant sites. Because individual fragments are short (~150 bp), we concatenated all loci into a supermatrix (Leaché & Oaks, 2017). Although a concatenated approach ignores the different coalescent histories of individual loci, each short ddRAD fragment contains limited phylogenetic information on its own, so concatenation is generally considered appropriate for ddRAD datasets (Eaton & Ree, 2013). We also note that, because the *M. ornatus–M. melanocephalus* clade is relatively young, we expect minimal issues with homology decay, as a large number of restriction sites should be orthologous across samples (Rubin et al., 2012). A full description of the RAXML-NG analyses is provided in the supplementary material (Text S5).

snapper: To infer evolutionary relationships among subspecies under a phylogenetic framework, we used snapper (Stoltz et al., 2021). Snapper infers a "species" tree using diffusion models and takes as input biallelic SNPs that are assumed to be unlinked, bypassing the necessity of building individual gene trees, similar to site-based coalescent methods (Bryant et al., 2012). To meet this assumption, we retained only a single SNP per RAD locus, thereby minimizing linkage among markers, and filtered loci based on missing data using a predetermined classification of individuals into populations (Table S3). A full description of the snapper analysis is provided in the supplementary material (Text S5).

OrientAGraph: As an alternative way to describe the historical relationships among subspecies, we used OrientAGraph (Molloy et al., 2021), an approach based on the TreeMix algorithm, which implements a graph-based model that uses genome-wide allele frequencies to infer population splits and admixture events (Pickrell & Pritchard, 2012). This method detects evidence of historical introgression between lineages and can better describe the history of populations when not fully bifurcating. A full description of the OrientAGraph analysis is provided in the supplementary material (Text S5).

Genetic structure within the *ornatus–melanocephalus* complex

PCA: To summarize genetic variation in the *ornatus–melanocephalus* complex, we conducted a genomic PCA using functions implemented in gdsfmt and SNPRelate (Zheng, 2013) in R. To conduct this PCA, we used only one SNP per locus, including only biallelic SNPs. To account for the effect of missing data on the PCA (Yi & Latch, 2022), we visualized the amount of missing data in our PC plots to evaluate the possibility that samples with high levels of missing data could be clustered together and/or have values biased toward the origin. When performing the PCA (*snpgdsPCA* function in *SNPRelate*), we also excluded SNPs with a missing rate higher than 0.1 (3,041 SNPs retained). We also conducted a PCA for a subset of the individuals to describe in more detail genetic variation in the hybrid zone and adjacent areas (*chrysops*, hybrid zone individuals, *bairdi*, and *griseonuchus*).

fineRADStructure: As a complementary approach to visualize genetic structure within the *ornatus–melanocephalus* complex, we used fineRADStructure, which estimates a coancestry matrix and an associated distance tree based on full haplotype information from RADseq data (Malinsky et al., 2018). This method has particularly high resolution for inferring recent shared ancestry, and allows the description of nested patterns of genetic structure (Malinsky et al.,

2018). To run *finestructure* (part of the fineRADStructure pipeline), we used the output from the populations program corresponding to full haplotype data (22,132 variant sites). No population prior was specified for the run, which was set for 200,000 iterations with a burn-in of 100,000 ($-x$ 100,000, $-y$ 100,000) and a thinning interval of 1,000 ($-z$ 1,000).

Calculation of F_{ST}: To estimate overall genetic differentiation between subspecies, we calculated pairwise F_{ST} between subspecies (i.e., plumage and geographic groups). We excluded all individuals from the hybrid zone from this analysis. Given the uncertainty regarding the *bairdi–griseonuchus* limits (see *Results* section), we also excluded individuals from the southern Ecuadorian provinces (as in the snapper analyses). We calculated the Weir and Cockerham estimator (Weir & Cockerham, 1984) using VCFtools (Danecek et al., 2011) in 25,000 bp windows. To test for potential discordance between nuclear and mitochondrial divergence, we evaluated whether SNP-based pairwise F_{ST} values were correlated with those estimated from the ND2 gene (Céspedes-Arias et al., 2021). To assess the correlation between these two matrices, we implemented a Mantel test based on Pearson's correlation using the function *mantel* implemented in the R package vegan (Oksanen et al., 2019).

To test for isolation-by-distance (IBD), we also calculated pairwise windowed F_{ST} between localities as defined in Table S1 and evaluated whether these were correlated with the pairwise geographic distances. Geographic distances between localities were calculated using the function *rdist.earth* implemented in the R package fields (Nychka et al., 2025). We also evaluated the correlation between these matrices using a Mantel test based on Pearson's correlation as implemented in vegan (Oksanen et al., 2019).

Admixture: We employed admixture (Alexander et al., 2009) to estimate individual genetic ancestries using a maximum-likelihood approach at three different geographic scales: the whole complex, the hybrid zone and adjacent populations (*bairdi*, *chrysops*, hybrid zone, *griseonuchus*), and the hybrid zone only (*bairdi*, *chrysops*, hybrid zone). Details on the admixture analysis are provided in the Supplementary Material (Text S6).

Fast Estimation of Effective Migration Surfaces: To more directly evaluate how genetic variation is shaped across the Andes, we used a spatially explicit model-based approach: Fast Estimation of Effective Migration Surfaces (FEEMS; Marcus et al., 2021) (https://github.com/VivaswatS/feems). This approach is based on a model of IBD and builds continuous migration surfaces based on a geographic grid, visualizing areas of inferred low and high gene flow (Marcus et al., 2021). Additional details on this analysis are provided in the Supplementary Material (Text S7).

Analysis of genetic variation across the *bairdi* × *chrysops* hybrid zone

Calculation of a genomic hybrid index and genetic composition of the hybrid zone

We estimated a genomic hybrid index and interclass heterozygosity using functions implemented in triangulaR (Wiens & Colella et al., 2025). As noted above, the southern parental population was defined based on our own results and includes individuals from central to southern Ecuador that do not cluster genetically with *griseonuchus* (see *Results* section). In the SNP dataset for this analysis, we included all SNPs per locus.

To identify ancestry-informative SNPs, we chose an allele frequency difference of 0.5 between parental populations. Higher thresholds resulted in very few (i.e., less than 10) or no SNPs being retained, and there were no alleles fixed in each parental population. Then, to describe the genetic composition of the hybrid zone, we used the values of genome-wide hybrid indices and observed interclass heterozygosity values for all individuals, and plotted these in a triangle plot (Cronemberger et al., 2020; Liu et al., 2022; Lopez et al., 2021).

Geographic cline analyses

To describe the geographic extent of the hybrid zone and evaluate whether genetic and plumage variation were concordant, we fitted geographic clines using HZAR v0.2-5 (Derryberry et al., 2014). We fitted and compared clines of genomic hybrid indeces—corresponding to admixture proportions—and plumage hybrid indices estimated previously for these individuals (Céspedes-Arias et al., 2021). For this analysis, we only included individuals ($n = 103$) with both genomic and plumage data, collected from localities with a sample size of four or more individuals. For each of these "traits," we fitted a model that estimates cline width (w) and center (c) but has fixed values for the mean and variance of the trait values at the cline extremes (μL, μR, $varL$, $varR$). Both models were run with a tune value of 1.5, and for each of these, we ran 3 chains of 2 million iterations discarding the first 10% as burn-in. All runs were performed randomizing starting parameters. To evaluate whether plumage and genomic hybrid index (i.e., genetic ancestry) clines are coincident and concordant, we compared the 95% confidence interval (CI) of the center and width estimates, which were calculated by aggregating the three independent chains for each model.

Results

Evolutionary relationships among subspecies as inferred from phylogenies and admixture graphs

We employed two different phylogenetic approaches to describe evolutionary relationships among the seven subspecies within the *M. ornatus–melanocephalus* complex. Using a maximum-likelihood approach with all loci concatenated, we found that most individuals of the same subspecies clustered together (Figure 1, panel C), yet we did not observe complete reciprocal monophyly in most groups. The *chrysops* group was the exception, as it appeared as a clade nested within the *ornatus* population. Notably, however, support values were generally low, implying that not many sites are phylogenetically informative as expected for a scenario of recent divergence and/or ongoing gene flow. Generally, we observed that individuals from geographically adjacent subspecies are intermixed in the tree.

The snapper subspecies-level tree (Figure 2A) showed strong support (posterior probability = 1.0, Figure S4) for a monophyletic "southern" group, encompassing three *M. melanocephalus* subspecies (*malaris*, *melanocephalus*, *bolivianus*) characterized by having spectacles and a black crown. The taxon *griseonuchus*, from north of the Marañón

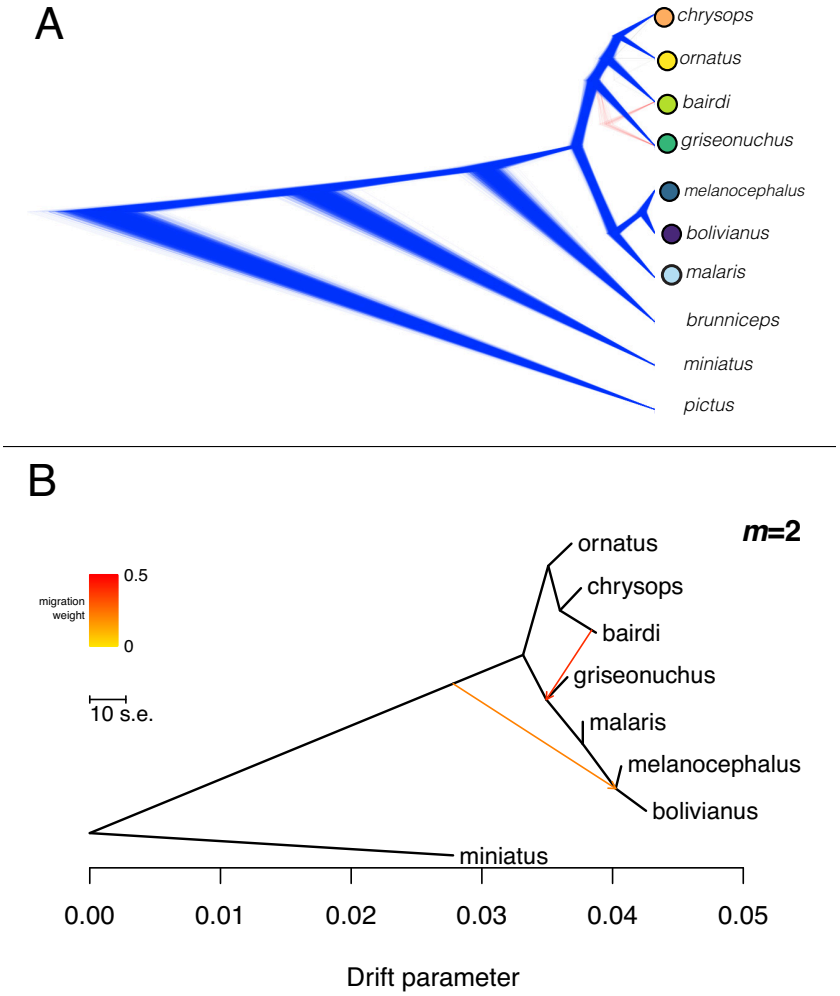

Figure 2. Evolutionary relationships among taxa in the *Myioborus ornatus–melanocephalus* complex as inferred by snapper and OrientAGraph. (A) DensiTree representation of the posterior distribution of trees from snapper. The blue lines represent the most frequent topology, while red and gray lines indicate less frequent topologies. (B) Admixture graph inferred by OrientAGraph with two migration edges. Migration edges are shown as colored arrows, with the hue indicating the migration weight.

River Valley, characterized by having a reddish crown that is phenotypically very similar to *bairdi*, was recovered as sister to a clade including the more northerly groups from Colombia and Ecuador. Within this expanded "northern" group, *chrysops* was recovered as sister to *ornatus*, and these, in turn, are sister to *bairdi* (Figure 2A). Note that, unlike the maximum-likelihood tree, we a priori assigned individuals to groups for these analyses, which can bias the phylogenetic estimation given that the limits among these populations are not fully defined.

We present here OrientAGraph admixture graphs based on models with $m = 1$ and 2 migration edges (Figure 2B, Figure S5). Because model likelihood plateaued at $m = 2$, we focus our discussion on this graph (Figure S6). Both OrientAGraph topologies recovered a monophyletic "southern" group (*malaris*, *melanocephalus*, and *bolivianus*), as seen in the snapper tree. However, in contrast to the snapper topology, both graphs recover *griseonuchus* as sister to this "southern" group. In both graphs, a *chrysops–bairdi–ornatus* group is inferred. The two hybridizing taxa, *bairdi* and *chrysops*, are recovered as sister in the $m = 2$ graph, while in the $m = 1$ graph *chrysops* is recovered as sister to its conspecific *ornatus* (Figure 2B, Figure S5).

The $m = 2$ graph (Figure 2B) indicates evidence of admixture between *bairdi* and *griseonuchus*, as indicated by the high migration weight of this edge. Another migration edge, with lower weight, was inferred between the branch leading to the ingroup and the *bolivianus–melanocephalus* group. This migration edge was also inferred in the $m = 1$ graph (Figure S5) and may reflect a signature of historical introgression between ancestral lineages within this species complex.

Genetic structure within the *ornatus–melanocephalus* complex

The PCA showed that individuals generally cluster in relation to plumage groups and geographic origin (Figure 3), but some phenotypically distinct groups were very close in the PC1-2 space (particularly *chrysops*, *ornatus*, and *bairdi*). As in the phylogenetic analyses, the "southern" group can be clearly distinguished, including all individuals from pop-

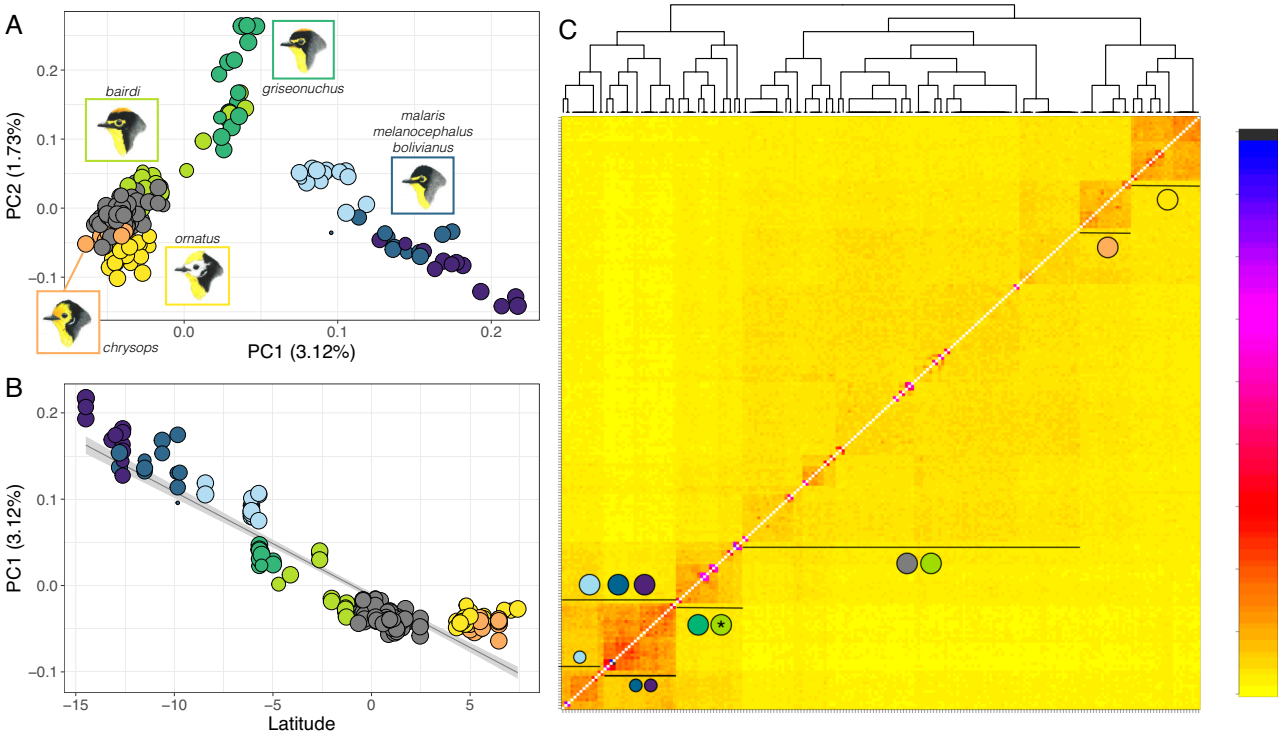

Figure 3. Genetic structure within the *ornatus–melanocephalus* complex. (A) The distribution of individuals in the PC1-2 space showing clustering based on plumage groups (i.e., subspecies), which are denoted by the color of the dots. (B) Strong correlation between PC1 and latitude. In both cases (A and B), dot size is inversely proportional to the amount of missing data. (C) fineRADStructure coancestry matrix, and associated distance tree (above) showing clusters that largely correspond to subspecies, which are denoted by the colors as in Figure 1 (showing hybrid zone birds in gray here). The asterisk highlights a small number of individuals putatively assigned to *bairdi*, all from the south end of Ecuador, that genetically cluster with *griseonuchus* (from northern Peru). The color scale denotes values of coancestry, with blueish tones corresponding to very high levels of coancestry. Subspecies are colored as follows: *bolivianus* (purple), *melanocephalus* (dark blue), *malaris* (light blue), *griseonuchus* (aquamarine), *bairdi* (lime green), hybrid zone individuals (gray), *chrysops* (orange), and *ornatus* (yellow).

ulations south of the Marañón River Valley (*bolivianus*, *melanocephalus*, *malaris*), which occupied a wide range of PC1 values (Figure 3A). When PC1 was plotted against latitude, a clear north–south pattern was revealed. There was also an identifiable northern cluster (*chrysops*, *bairdi*, and hybrid zone individuals) that was, however, not fully distinct from a third cluster comprised of *griseonuchus* individuals. Within this northern cluster, the subspecies *ornatus*, *chrysops*, *bairdi*, and individuals from the hybrid zone ("northern," hereafter) appeared very close in PC1-2 space. As expected, individuals from the hybrid zone (in gray in Figure 3) fell intermediate between their parental populations. The *ornatus* group appeared as a more defined cluster when considering PC3 (Figure S7). Notably, some individuals putatively classified as *bairdi*, collected in the Ecuadorian provinces of Loja and outlying ridges in the Amazon, appeared to cluster with *griseonuchus* (Figure 3). We observed a similar pattern in the hybrid zone plus *griseonuchus* PCA (Figure S8).

Two main clusters are supported in the coancestry matrix resulting from fineRADstructure: populations occurring from north Peru Dto Bolivia (*griseonuchus* plus "southern" group), and those occurring from Ecuador to Colombia ("northern" group) (Figure 3C), which contrasted with the topology inferred by snapper. Within the first group, *griseonuchus* and the southern group appear as differentiated clusters. The few exceptions to this pattern are a few putatively *bairdi* individuals that clustered with *griseonuchus*, which were collected at the southern edge of the distribution of this subspecies (where it is replaced by *griseonuchus*) in the Cordillera del Cutucú and Loja Province of Ecuador. We detected two main groups within the "northern" group (Ecuador and Colombia): one corresponded to *ornatus* and *chrysops*, and the other to *bairdi* and individuals from the hybrid zone.

Admixture analyses, including all individuals in the *ornatus–melanocephalus* complex, revealed genetic breaks along the distribution of these warblers that were overall consistent with fineRADStructure (Figure 4A). For example, when assuming $K = 2$ and $K = 3$, the "southern" group appeared as an identifiable cluster. For $K = 2$, which is the optimal K value based on cross-validation error values (Figure S9, top panel), the group *griseonuchus* also clustered with the southern group (Figure 4A). For $K = 3$, a "southern" plus *griseonuchus* group can be also identified, and there was an additional genetic break roughly located in the described *bairdi* × *chrysops* hybrid zone in southern Colombia (see Figure 1A). For both K values, replicate runs were highly concordant (average pairwise similarity = 0.99 in both cases), with pong recovering a single clustering mode.

The results of admixture analyses focused on the hybrid zone and parental populations, when assuming $K = 2$, showed a genetic break that clearly coincides with the *bairdi* × *chrysops* hybrid zone (Figure 4B3 and C3), as previously identified based on plumage variation (Figure 1A). However, when also considering *griseonuchus*, the transition

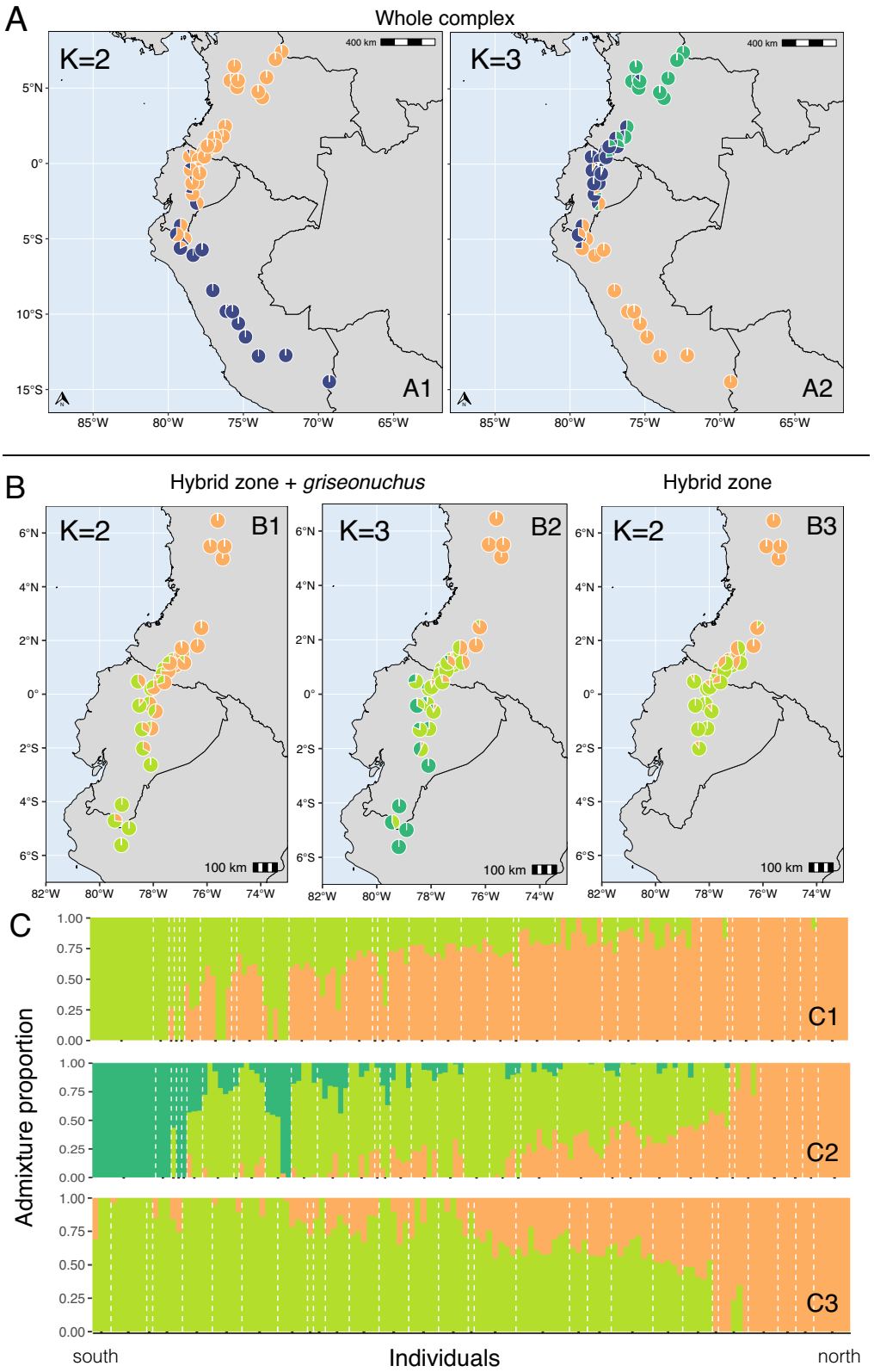

Figure 4. Genetic clusters (A) across the entire distribution of the *ornatus–melanocephalus* complex and (B) the hybrid zone and adjacent populations as shown by the mean admixture proportions per locality. The dataset and *K* value for each plot are specified at the top of each map. (C) Admixture proportion barplots showing the admixture proportions per individual, organized by localities from south to north (localities are divided by white dashed lines).

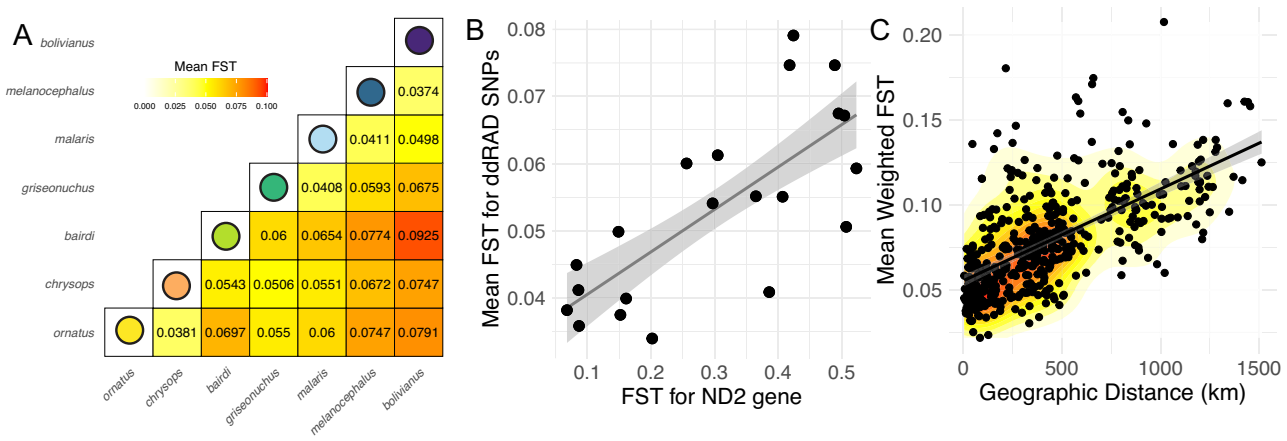

Figure 5. Genetic differentiation among Andean *Myioborus* taxa. (A) Mean pairwise F_{ST} values between subspecies (i.e., geographically circumscribed plumage groups). (B) Correlation between pairwise F_{ST} calculated with ddRAD SNPs (this study) and the ND2 mitochondrial gene from the same set of samples (Céspedes-Arias et al., 2021). (C) Positive correlation between geographic distance and F_{ST} between localities supports a role of isolation-by-distance shaping genetic variation in the *ornatus–melanocephalus* complex.

between these genetic groups is less sharp and displaced to the south (Figure 4B1). When using $K = 3$ for the analyses including *griseonuchus* (a K that corresponds to the number of subspecies), two genetic clusters were identified in Ecuador, and one in Colombia, and one of these genetic breaks did again roughly correspond to the *bairdi* × *chrysops* hybrid zone (Figure 4B2). In both cases, the K value with the lowest cross-validation is $K = 1$ (Figure S8). For both analyses (including and excluding *griseonuchus*), pong identified a single clustering mode across all evaluated K values ($K = 2$ for the hybrid zone analysis; $K = 2$ and 3 for the analysis, including *griseonuchus* and southern *bairdi* populations). Replicate runs were highly concordant, with mean pairwise similarity >0.95 in all cases.

Values of pairwise F_{ST} between populations showed an overall correspondence with geographic distance: subspecies that are far apart in space show higher genetic differentiation (e.g., *bairdi* vs. *bolivianus*, Figure 5). We observed higher pairwise differentiation between taxa belonging to the "southern" versus "northern" groups, which is consistent with all other analyses describing genetic structure. In contrast, there was very low differentiation among the three subspecies occurring south of the Marañón River Valley ("southern" group), which all have similar head coloration. However, there were also relatively low levels of differentiation within the "northern" plus *griseonuchus* group, which encompasses striking plumage diversity, particularly between the two hybridizing taxa, *bairdi* and *chrysops*, and *bairdi* and *griseonuchus* (Figure 5). There was a positive correlation (Figure 5, Mantel statistic $r = 0.75$, p-value = .001) between pairwise F_{ST} calculated from our ddRAD SNPs and from the ND2 mitochondrial gene (Céspedes-Arias et al., 2021). Lastly, as expected, if patterns of genetic variation reflect IBD, we found a positive correlation between pairwise F_{ST} between localities and geographic distance (Figure 5, Mantel statistic $r = 0.65$, p-value = .001). Using the same classification scheme for individuals as that used to calculate F_{ST}, we estimated genetic diversity statistics. We found that nucleotide diversity is very similar among groups, ranging from 0.00218 to 0.0027 (Table S4).

The migration surfaces inferred by FEEMS indicate spatial heterogeneity in effective migration across the distribution of these warblers, highlighting regions where gene flow is reduced relative to the surface's mean (Figure 6). These areas of low migration coincided mostly with two geographic breaks that dissect the distribution of the complex (Figures 1 and 6), specifically the Magdalena River Valley and the Marañón River Valley, and with the hybrid zone. In contrast, most of the range south of the North Peruvian Low

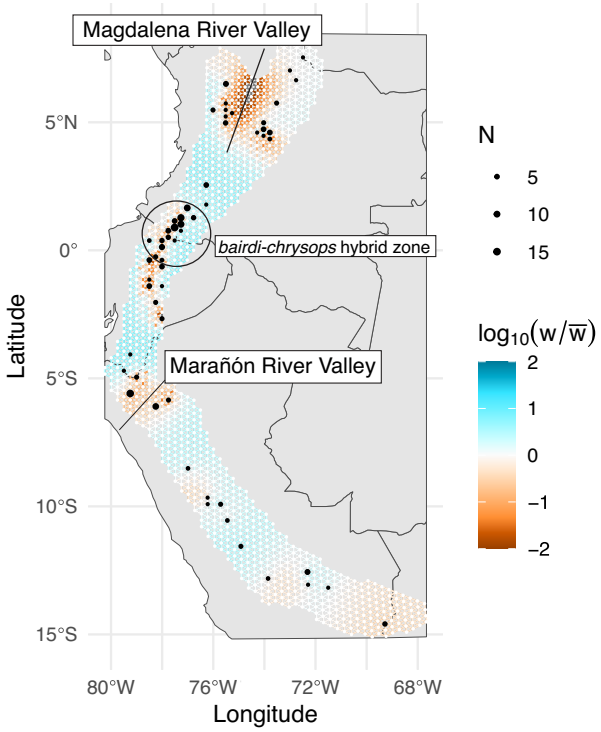

Figure 6. Estimated effective migration graph across the entire distribution of the *Myioborus ornatus–melanocephalus* complex, highlighting areas of restricted gene flow. The edges of the grid are colored by estimated effective migration, from burnt orange (low migration) to blue (high migration). In the grid, the black dots correspond to the sampled nodes, and the size of the dots corresponds to the sample size (M). We highlight three areas of low migration, two geographic barriers, and the hybrid zone where genetically distinct taxa have come into contact.

shows moderate to high inferred effective migration, with no clear spatial discontinuities, consistent with genetic structure that is broadly explained by a relatively homogeneous IBD process.

We acknowledge that low sampling density in certain regions, particularly in southern Ecuador and central and southern Peru, may have influenced the inferred migration surface (Figure 6). However, cross-validation results indicate that the selected regularization parameter provides a good fit while accounting for unobserved nodes (Figure S10). With that caveat in mind, the FEEMS results are broadly consistent with the patterns of genetic structure revealed by our other analyses.

Hybrid zone

To describe the geographic extent of hybridization and the genetic composition of the *bairdi* × *chrysops* hybrid zone, we identified ancestry-informative markers to estimate genomic hybrid indexes and interclass heterozygosity for individuals across the hybrid zone and parental *bairdi* and *chrysops* populations. Using a relatively low threshold for allele frequency difference (0.5), we identified only 29 sites that were ancestry informative from the total of 14,301, and none of these were fixed between the parental populations. This result complicates the interpretation of the triangle plots and highlights the low level of genetic differentiation between these two hybridizing taxa. Because of the scarcity of ancestry informative sites in our ddRAD data set, which can affect the accuracy of genomic hybrid index estimations, we opted to conduct cline analyses with admixture proportions (with $K = 2$) instead.

We found that the geographic clines of head coloration and genomic hybrid index (i.e., genetic ancestry), defined as the admixture proportions in Figure 4 (panel C3) had different centers but similar widths (Figure 7, panel A). The admixture proportion cline had a width of 281.6 km (95% CI: 245.0−319.8 km), compared to 240.6 km for head coloration (95% CI: 277.5−311.1 km). Given the substantial overlap in CIs, we do not interpret this 41 km difference in width as significant. However, we found a 38 km difference in the estimates of the geographic center between the plumage and genetic ancestry, for which the 95% CIs did not overlap. For genetic ancestry, the cline was centered around 348.8 km (95% CI: 335.4−362.7 km) in our sampling transect, while the plumage cline was centered around 311.1 km (95% CI: 300.7−322.6 km). Therefore, based on our HZAR analyses, the plumage cline appeared to be displaced toward the south (i.e., toward Tungurahua, Ecuador, southern extreme of the sampling transect), implying that the *chrysops*-like plumage traits may be introgressing into *bairdi*. However, there was an overall strong correlation between the plumage hybrid indices and genetic ancestry across the hybrid zone and allopatric populations (Figure 7, panel C; linear model; p-value $< .001$, $m = 0.9$, R-squared $= 0.8$). We identified the outliers of this linear regression as those individuals with residuals >2 SD units from the mean, finding that most were below the regression line (Figure 7). Specifically, we identified six individuals that had a more *chrysops*-like plumage from the hybrid zone area (i.e., lower) relative to what the model predicts based on the admixture proportion, which was consistent with the cline analysis results that show that *chrysops*-like plumage is introgressing into *bairdi*.

To describe the genetic composition of the *bairdi* × *chrysops* hybrid zone, we built triangle plots (interclass heterozygosity vs. hybrid index) based on the 29 ancestry-informative markers that we identified (Figure 7, panel D). The individuals from the hybrid zone are distributed toward the center of the triangle, many below the line that defines what value combinations are possible under Hardy–Weinberg equilibrium, which is likely a product of the low allele frequency difference threshold. We note that individuals from populations away from the hybrid zone (Figure 7, in green and orange) are not located in the bottom corners of the triangle plot, which is expected given that the allele frequency difference threshold is lower than one. If interpreted considering the caveats described above, the distribution of individuals in the triangle is suggestive of a hybrid zone mostly composed of advanced generation hybrids, without many F1s.

Discussion

We used reduced-representation genomic data to study genetic variation at two different spatial scales: the full distribution of a geographically variable warbler complex (*M. ornatus–melanocephalus*) and a known hybrid zone between two of these plumage forms. At both scales, our set of thousands of SNPs allowed us to explore genetic structure with a resolution that mtDNA loci could not provide in previous studies (Céspedes-Arias et al., 2021; Pérez-Emán, 2005). We found evidence of IBD driving genetic structure across the latitudinally extensive range of these warblers, and genetic divergence increasing where ranges are separated by known geographic barriers (i.e., Magdalena and Marañón river valleys; Gutiérrez-Pinto et al., 2012; Martínez-Gómez et al., 2023; Winger & Bates, 2015). These clear genetic breaks coincided with observed differences in head plumage coloration among populations. One transition corresponds to a hybrid zone between *bairdi* and *chrysops*, likely composed primarily of advanced-generation hybrids, where variation in genetic ancestry correlates with head coloration.

Below, we discuss how our findings relate to the history of divergence and gene flow among these populations, with a focus on how genetic variation imperfectly covaries with plumage traits, and how it is structured across geography. We then discuss how genetic variation is structured across the hybrid zone, how it relates to patterns of variation in head coloration in this area, and whether there is evidence of selection against hybrids maintaining this seemingly extensive hybrid zone.

Geographic variation in plumage color and genetic structure

Our qualitative assessments based on historical plumage descriptions and examinations of study skins suggest that for these *Myioborus*, patterns of geographically clustered phenotypic variation coincide with phylogeographic structure. First, we found that individuals belonging to the same subspecies usually form genetic clusters, and that all major genetic breaks within the species complex coincide with a transition between clearly differentiated plumage groups, although we note that we lack data quantifying the degree of plumage differentiation between subspecies (e.g.,

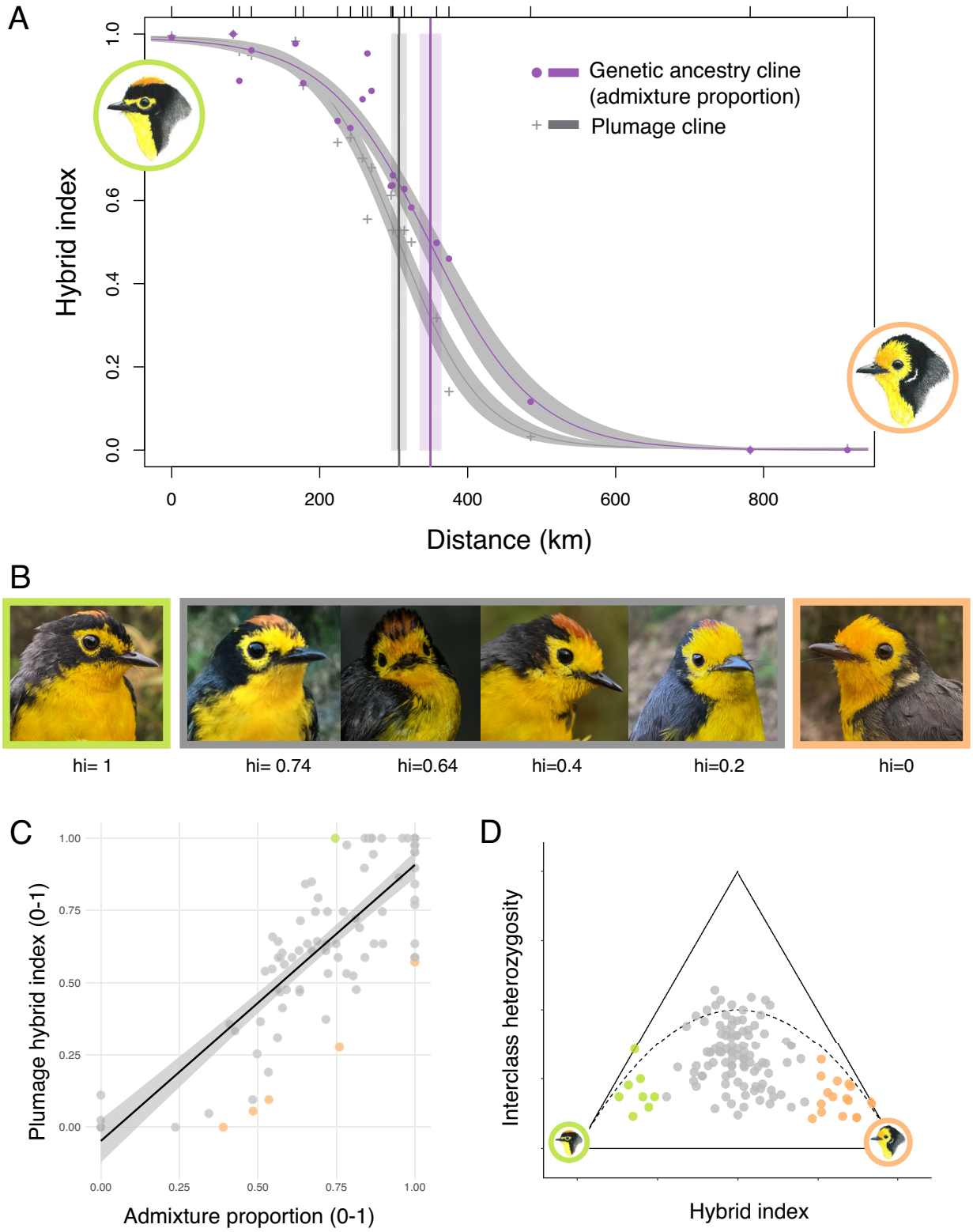

Figure 7. Genetic and plumage variation across the *bairdi* × *chrysops* hybrid zone. (A) The plumage and genetic ancestry geographic clines have different estimated centers. (B) Photographs of birds collected for which we calculated a plumage hybrid index, showing a sample of the phenotypic diversity across the hybrid zone, and parental phenotypes at both extremes. (C) We observed an overall strong correlation between the genomic hybrid index (*bairdi* admixture proportion) and the plumage hybrid index. Most individuals that deviate from this relationship (outliers marked in color) are individuals with a more *chrysops*-like plumage than expected given the admixture proportion. (D) Triangle plot showing the genetic composition of the hybrid zone. The *x* axis corresponds to a genomic hybrid index as calculated using 29 ancestry-informative markers. Parentals are shown in lime green and orange. Photos: Andrés Cuervo, Paulo Pulgarín, David Ocampo, and Laura Céspedes Arias.

Winger & Bates, 2015). In addition, subspecies with seemingly subtle plumage differentiation (Cuervo & Céspedes-Arias, 2023), specifically those occurring south of the Marañón River Valley and all characterized by black crowns and spectacles, show little genetic differentiation from one another.

Previous examinations of genetic variation in mitochondrial loci (Céspedes-Arias et al., 2021; Pérez-Emán, 2005) found extensive haplotype sharing and little genetic differentiation among the subspecies *ornatus* and the hybridizing *bairdi* and *chrysops*, which are all characterized by striking plumage differences. In contrast, in our analyses of ddRAD data, which encompass thousands of SNPs across the genome, these subspecies are each identifiable genetic clusters, albeit with shallow genetic differentiation. Taken together, we interpret these results as evidence of rapid and recent diversification of head plumage patches in the *ornatus–melanocephalus* complex, as seen in other Neotropical taxa (Campagna et al., 2012, 2017). Our results also highlight the usefulness of reduced representation genomic data to study the evolutionary history of young radiations (Aguillon et al., 2018; Toews et al., 2016a; Wagner et al., 2013), in which few loci might be insufficient to detect genetic differentiation and describe evolutionary relationships among phenotypically distinct populations (Friis et al., 2016; Stryjewski & Sorenson, 2017). We note that lack of differentiation in mtDNA between phenotypically distinct groups could also be the result of mitochondrial introgression (Irwin et al., 2009; Toews & Brelsford, 2012), although the strong positive correlation of F_{ST} for ND2 and our ddRAD loci does not support a scenario of extensive mitochondrial introgression in the group.

Genetic structure in the region of the Andes spanning from central Ecuador to northern Peru (north of the Marañón River Valley) is complex and not clearly associated with a single topographic feature. This area also broadly corresponds to the transition between *bairdi* and *griseonuchus* plumage (Figure 1, Figure S1), two subspecies characterized by a rufous crown and spectacles. Despite their overall similarity, these two groups show differentiation in at least two head plumage traits: the presence of a black band behind the rufous crown and the extent of black in the cheeks and lores (Cuervo & Céspedes-Arias, 2023; Curson et al., 1994; Zimmer, 1949). Our qualitative assessments of plumage variation (Figure S1), however, suggest that the variation in these traits might not be completely discrete. Moreover, we found that individuals from Loja and the Cordillera del Cutucú (Ecuador) show substantial variation in both putatively diagnostic plumage traits. Therefore, these individuals, which are genetically clustered with *griseonuchus*, do not uniformly resemble the individuals from Cajamarca, Peru. Because of limited sampling in the area, we are unable to draw stronger conclusions, but our data suggest that there is some discordance between plumage and genetic variation, and evidence of introgression based on admixture graphs. Despite some differentiation in at least these two plumage traits, our genetic results are concordant with substantial historical or contemporary gene flow among populations in this area. This pattern suggests that the geographic range of *bairdi* is potentially outlined by two hybrid zones, one to the north with *chrysops* (Céspedes-Arias et al., 2021) and one to the south with *griseonuchus*. Evaluating this hypothesis of hybrid zones at the range edges, as observed in barn swallows (Scordato et al., 2017), will require a systematic collection of specimens across the *bairdi–griseonuchus* boundary.

Genetic structure across space: the influence of geographic distance and topographic features along the Andes

Several of our analyses support a strong correlation between genetic variation and geographic locations of samples and an important role of IBD driving genetic structure in *Myioborus* along the Andes. Patterns of IBD are close to ubiquitous in nature (Aguillon et al., 2017; Seeholzer & Brumfield, 2018; Vos & Velicer, 2008, but see Meirmans, 2012), and are often treated as a null expectation for genetic differentiation if organisms have limited dispersal given the scale of their range, as is the case for these small warblers with a latitudinally expansive distribution range.

However, spatially homogeneous IBD does not fully explain the observed patterns of genetic variation. Specifically, we found evidence of discrete genetic clusters and of reduced effective migration (relative to average genetic differentiation per unit geographic distance) in some regions of the Andes, which in turn correspond to lowland valleys such as the Marañón and the Magdalena River Valleys. These deep, lowland gaps interrupt the continuity of humid high-elevation forest and scrub (Graham et al., 2010) that these *Myioborus* inhabit in the present, and also coincide with genetic and phenotypic breaks within other taxa that inhabit similar elevation bands (Gutiérrez-Pinto et al., 2012; Martínez-Gómez et al., 2023; Winger & Bates, 2015). These two topographic features were also identified in a comparative study as being associated with allopatric events across multiple Andean bird genera (Hazzi et al., 2018). These genetic breaks, clearly tied to topographic features, also correspond with striking discontinuities in head coloration traits.

Other areas associated with clear genetic breaks observed in the inferred migration surface were not clearly associated with topographic features that interrupt the present-day continuity of humid, high-elevation forests. Specifically, low migration was inferred in a large area ranging from the border between Ecuador and Colombia down to southern Ecuador. We suggest that this pattern results partially because this broad area includes the *bairdi* × *chrysops* hybrid zone, in which genetic differentiation relative to distance is expected to be higher than what is expected under pure IBD, as two somewhat genetically distinct taxa came into secondary contact. The extension of this area of low inferred migration to south Ecuador is consistent with our fineRADStructure, PCA, and admixture results that suggest that there is substantial genetic differentiation between individuals in close geographic proximity in this area. Specifically, we found that birds from isolated mountain spurs such as the Cordillera del Cutucú (southeastern Ecuador) and Cordillera del Condor (Peru–Ecuador border) clustered genetically with birds from the main Andes in Cajamarca (northwestern Peru), and Loja (southern Ecuador), instead of the more geographically proximate individuals from the eastern Ecuadorian Andes in Morona–Santiago. The Cordillera del Cutucú and Cordillera del Cóndor are outlying mountain ranges in the Amazonian foothills, separated from the main Andes by the valleys of the rivers Upano and Zamora, respectively (Pozo-Zamora et al., 2022; Robbins et al., 1987). Our results suggest that these valleys,

and surrounding lowland areas, have likely acted as dispersal barriers for these high-elevation warblers. On the other hand, the patterns of genetic variation described here indicate that there has likely been substantial gene flow connecting the populations of warblers inhabiting isolated peaks in these mountain ranges (separated by the Santiago River Valley; Pozo-Zamora et al., 2022; Robbins et al., 1987), and the eastern slope of the Andes in northern Peru.

Hybrid zone dynamics

Based on our reduced-representation genomic data set, the hybridizing *chrysops* and *bairdi* are characterized by very shallow genetic divergence, which contrasts with their striking plumage differentiation. Moreover, across thousands of SNPs, we only identified 29 ancestry informative sites with substantial allele frequency differences between parental populations. This scarcity of ancestry informative markers limits our ability to draw definitive conclusions about the genetic composition of this hybrid zone but highlights the low level of genetic differentiation between *chrysops* and *bairdi*.

This hybrid zone likely formed by secondary contact of two formerly isolated plumage forms. The disconnection and subsequent reconnection of habitat that could have shaped this process may have followed elevational shifts in the cloud forest belt during the Pleistocene (Flantua et al., 2014; Ramírez-Barahona & Eguiarte, 2013), or potentially been driven by volcanic activity that modified topographic connectivity (Sanín et al., 2024). An investigation of the evolutionary origins of this hybrid zone will require both a better understanding of the patterns of connectivity of cloud forest in the area where it is centered, as well as an estimation of the time since secondary contact, which could be obtained from whole genome data through demographic modeling based on allele counts (Excoffier et al., 2013) or inferences based on ancestry tract lengths (Pool & Nielsen, 2009).

Our geographic cline analyses using plumage and genomic data suggest that the hybrid zone extends for over 200 km, similar to the findings from its original description based on face color traits (Céspedes-Arias et al., 2021). We do not find statistically significant differences in the width of the admixture proportion (i.e., genomic) and plumage geographic clines. Taken together, plumage and genomic patterns of variation thus suggest that hybridization between *chrysops* and *bairdi* has been extensive, albeit still restricted to a fraction of the entire distribution of these taxa (approximately 30% of our sampling transect), which is continuous at least from central Ecuador to the north of the Central Andes of Colombia. Therefore, the geographic extent of hybridization is unlikely to be constrained by physical or ecological barriers that limit dispersal beyond the hybrid zone (e.g., DeRaad et al., 2023), raising the question of what factors are restricting the hybrid zone to this area.

The lack of information on natal dispersal distances as well as the wide range of plausible times since secondary contact constrains our ability to generate a direct comparison of the observed cline widths with that expected under neutral diffusion (Barton & Gale, 1993). With the available data, we are thereby unable to evaluate whether the *chrysops* × *bairdi* hybrid zone corresponds to a stable tension zone, in which the width of clines is constrained by selection against hybrids. A second possibility is that the observed sharp genomic and plumage clines are not maintained by selection, but instead that this is a young and potentially expanding hybrid zone, and that the differentiation between *chrysops* and *bairdi* might become eroded over time (Kearns et al., 2018).

Using a range of plausible dispersal distances inferred (Mumme, 2015), we can approximate expectations under neutrality (Barton & Gale, 1993). For a cline width of 281 km, the neutral diffusion model predicts that ~14,337 generations would be required assuming a dispersal distance of 935 m, or ~53,278 generations with a dispersal distance of 485 m. In principle, building upon our systematic collection of specimens across the *chrysops* × *bairdi* hybrid zone, the alternative of an expanding hybrid zone could be revisited by comparing geographic clines of plumage and genomic hybrid indices, based on specimens collected across different time points. However, given that the expansion of this hybrid zone under neutral diffusion with plausible dispersal distances is expected to be slow (i.e., 0.5 km over 50 generations), time between sampling periods would need to be very long to detect changes.

We found that cline centers are not fully coincident, as that of the plumage cline is displaced to the south of the genetic ancestry cline center, implying that the *chrysops*-like plumage is introgressing into *bairdi*. Assuming that most of our ddRAD loci can be considered neutral markers, our results indicate that head coloration might be under selection across this hybrid zone (Gay et al., 2008). Specifically, the observed pattern would be consistent with a scenario in which the *chrysops*-like plumage is favored across the hybrid zone, which would lead to the asymmetric introgression of this phenotype toward the south. Asymmetric introgression of plumage traits has been observed in other avian hybrid zones (Baldassarre et al., 2014; Del-rio et al., 2022; DeRaad et al., 2023; Lim et al., 2024; Semenov et al., 2021), and in at least two of these cases, behavioral evidence supported the idea that these traits provide fitness advantages in the context of mate choice (Baldassarre & Webster, 2013; Long et al., 2024; Stein & Uy, 2006a).

Even though the difference in plumage and genetic ancestry center is statistically significant, we found it to be relatively small (38 km; approximately 4% of the entire sampling transect). This contrasts with much more marked differences in center estimations found in other hybridizing birds like *Motacilla* wagtails (Semenov et al., 2021) and *Malurus* fairy-wrens (Baldassarre et al., 2014). We acknowledge that this minor difference could be an artifact of the way in which both of our hybrid indexes were calculated (e.g., with the scoring system giving equal weight to predefined patches; Céspedes-Arias et al., 2021), and potentially low sampling sizes in some of the localities. However, this slight difference could be the result of selection on the head plumage patches. Even though the role of these color patches has not been studied in these warblers yet, it is plausible that they may be relevant for intraspecific communication and mate choice as seen in head plumage patterns in many other bird species (e.g., Andersson et al., 1998; Marchetti, 1992; Rémy et al., 2010; Scott & Deag, 1998). Future behavioral studies (e.g., taxidermic mount presentation experiments; Avendaño, 2021; Ocampo et al., 2025; Uy et al., 2009) could evaluate these hypotheses of selection favoring *chrysops*-like head color patterns across this hybrid zone.

Besides describing the geographic extent of hybridization, we used our reduced-representation genomic data set to gain insights into the genetic composition of the *chrysops* × *bairdi* hybrid zone. However, as noted above, the scarcity of ancestry informative sites in our dataset complicates the interpretation of these results, as it compromises the accuracy of genomic hybrid indexes and interclass heterozygosity estimations (Gompert et al., 2024; Wiens & Colella et al., 2025). Setting a low allele frequency threshold, which was necessary in our case, can also result in a tendency of individuals to cluster near the center of triangle plots (Wiens & Colella et al., 2025). Bearing these caveats in mind, we interpret our triangle plot results as suggestive of a hybrid zone composed mostly of advanced generation hybrids, with no F1s sampled, given the lack of individuals with intermediate hybrid indexes and very high interclass heterozygosity (Capblancq et al., 2020; DeRaad et al., 2023; Natola et al., 2021). This is consistent with the existence of a high diversity of plumage phenotypes in the hybrid zone, as well as the lack of contemporary geographic contact between parental *chrysops* and *bairdi* populations (i.e., we do not observe "pure" individuals of both species in the same sites) (Céspedes-Arias et al., 2021). Given the shallow genetic divergence between *chrysops* and *bairdi*, a more detailed examination of the genetic composition of this hybrid zone will necessitate whole-genome sequencing, capturing more ancestry informative sites. Specifically, as in other examples of hybridizing taxa with very little genomic divergence, whole-genome sequencing may be needed to identify regions and sites that are highly differentiated and allow hybridization dynamics to be studied in detail (Aguillon et al., 2021; Poelstra et al., 2014; Toews et al. 2016b).

Supplementary material

Supplementary material is available online at *Evolution*.

Data availability

All the scripts used to conduct analyses and produce figures are available in a GitHub repository (https://github.com/lcespedesarias/myioborus-genomics). Raw genetic data are available in the NCBI SRA database (PRJNA1423728). The VCF files used as input for analyses are available in a Dryad repository (doi: 10.5061/dryad.msbcc2gck).

Author contributions

L.N.C.A, A.M.C., C.D.C., and L.C. conceived the study; L.N.C.A. and A.M.C. conducted fieldwork with substantial logistical support from C.D.C. and E.B.; C.W. contributed tissue samples; L.N.C.A. conducted lab work with support from L.C. and I.L.; L.N.C.A. conducted the bioinformatic processing of data and data analyses with substantial input from L.C. L.N.C.A. wrote the original draft, with major contributions from L.C. All authors contributed to reviewing and editing the manuscript.

Funding

This project had the financial support of the Society of Systematic Biologists (Graduate Student Research Award to L.N.C.A.), Association of Field Ornithologists (Bergstrom Award to L.N.C.A.), Neotropical Ornithological Society (François Vuilleumier Fund to L.N.C.A.), National Geographic Society (Young Explorers Grant WW-R014-17 to L.N.C.A. and Support for Women + Dependent Care grant to L.N.C.A.) and the Fuller Evolutionary Biology program of the Cornell Lab of Ornithology. The participation of L.N.C.A. in the 2024 Workshop on Genomics, which was instrumental to conduct analyses presented here, was funded by The University of Chicago (Steiner Award and D&I Small Grants of the Biological Sciences Division).

Conflict of interest

The authors declare no conflicts of interest.

Acknowledgments

We are grateful to Bronwyn Butcher for supporting our work at the Fuller Evolutionary Biology Lab (Cornell Lab of Ornithology). We thank the following people for contributing to fieldwork across the *bairdi x chrysops* hybrid zone, which resulted in the collection of most specimens included here: P. Montoya, D. Céspedes Arias, P. Pulgarín, F. González, E. Obando, M.A. Meneses, and D. Ocampo. Our fieldwork was made possible by many landowners, local guides, nature reserve officials, and other members of local communities who allowed us access to their land, contributed with invaluable logistical support and even welcomed us warmly into their homes. We are grateful to the Universidad de los Andes, particularly Mireya Osorio, and to the Universidad Tecnológica Indoamérica for their crucial support in obtaining export permits. Collecting and export from Ecuador (Contrato de Acceso a Recursos Genéticos MAE-DNB-CM-2015-0017 and No. 40-2018-EXP-CM-FAU-DNB/MA to the Universidad Tecnológica de Indoamérica); Colombia (Number 01374 to the Universidad de los Andes). See Céspedes-Arias et al. (2021) for information on collecting permits. We are also grateful to museum collections that provided tissue loans to conduct this study: Museum of Southwestern Biology, Kansas University Natural History Museum, LouisianaState University Museum of Natural Science, Pontificia Universidad Católica del Ecuador, Instituto de Investigación de Recursos Biológicos Alexander von Humboldt, Universidad de los Andes, and the Cornell University Museum of Vertebrates. We thank Nathan Rice, Jason Weckstein (ANSP), Sebastian C. Perez, Nicholas Mason (LSUMZ) and Santiago Burneo(QCAZ) for providing photographs of museum specimens. We also thank Shannon Hackett, John Bates, Ben Marks (FMNH), Socorro Sierra and Gustavo Bravo (IavH) for facilitating the examination of study skins. For computing cluster access and technical support, we thank the High-Performance Computing Center at Cornell University (BioHPC) and The University of Chicago Center for Research Informatics. We thank Josie Paris for general advice on Stacks use, Stepfanie Aguillon for suggestions on phylogenetic analyses, and Erin Molloy for advice on the use of OrientAGraph. For helpful discussions, L.N.C.A. thanks the Lovette lab group, as well as Abhimanyu Lele, Santiago Herrera, John Bates, Trevor D. Price, Marcus Kronforst, John Novembre, and Pavitra Muralidhar. We are very grateful to Andrés Montes Rojas for providing the *Myioborus* illustrations used here. Lastly, we would like to thank the two anonymous reviewers and the Associate

Editor Scott Taylor for their insightful comments and suggestions, which substantially improved our manuscript.

References

Abbott, R. J., Barton, N. H., & Good, J. M. (2016). Genomics of hybridization and its evolutionary consequences. *Molecular Ecology*, *25*(11), 2325–2332. https://doi.org/10.1111/mec.13685

Aguillon, S. M., Campagna, L., Harrison, R. G., & Lovette, I. J. (2018). A flicker of hope: Genomic data distinguish Northern Flicker taxa despite low levels of divergence. *The Auk*, *135*(3), 748–766. https://doi.org/10.1642/AUK-18-7.1

Aguillon, S. M., Fitzpatrick, J. W., Bowman, R., Schoech, S. J., Clark, A. G., Coop, G., & Chen, N. (2017). Deconstructing isolation-by-distance: The genomic consequences of limited dispersal. *PLoS Genetics*, *13*(8), 1–27. https://doi.org/10.1371/journal.pgen.1006911

Aguillon, S. M., Walsh, J., & Lovette, I. J. (2021). Extensive hybridization reveals multiple coloration genes underlying a complex plumage phenotype. *Proceedings of the Royal Society B: Biological Sciences*, *288*(1943), 20201805. https://doi.org/10.1098/rspb.2020.1805

Alexander, D. H., Novembre, J., & Lange, K. (2009). Fast model-based estimation of ancestry in unrelated individuals. *Genome Research*, *19*(9), 1655–1664. https://doi.org/10.1101/gr.094052.109

Andersson, S., örnborg, J., & Andersson, M. (1998). Ultraviolet sexual dimorphism and assortative mating in blue tits. *Proceedings of the Royal Society of London. Series B: Biological Sciences*, *265*, 445–450. https://doi.org/10.1098/rspb.1998.0315

Andrews, S. (2010). *FastQC: A quality control tool for high throughput sequence data*. http://www.bioinformatics.babraham.ac.uk/projects/fastqc. Accessed July, 2019.

Avendaño, J. E., & Cadena, C. D. (2021). Territorial males do not discriminate between local and novel plumage phenotypes in a tropical songbird species complex : Implications for the role of social selection in trait evolution. *Behavioral Ecology and Sociobiology*, *75*, 37. https://doi.org/10.1007/s00265-021-02972-0

Baiz, M. D., Wood, A. W., Brelsford, A., Lovette, I. J., & Toews, D. P. L. (2021). Pigmentation genes show evidence of repeated divergence and multiple bouts of introgression in *Setophaga* warblers. *Current Biology*, *31*(3), 643–649.e3. https://doi.org/10.1016/j.cub.2020.10.094

Baldassarre, D. T., & Webster, M. S. (2013). Experimental evidence that extra-pair mating drives asymmetrical introgression of a sexual trait. *Proceedings of the Royal Society B: Biological Sciences*, *280*(October), 1–7. https://doi.org/10.1098/rspb.2013.2175

Baldassarre, D. T., White, T. A., Karubian, J., & Webster, M. S. (2014). Genomic and morphological analysis of a semipermeable avian hybrid zone suggests asymmetrical introgression of a sexual signal. *Evolution*, *68*(9), 2644–2657. https://doi.org/10.1111/evo.12457

Barker, K., Burns, K. J., Klicka, J., Lanyon, S. M., & Lovette, I. J. (2015). New insights into New World biogeography: An integrated view from the phylogeny of blackbirds, cardinals, sparrows, tanagers, warblers, and allies. *The Auk*, *132*(2), 333–348. https://doi.org/10.1642/AUK-14-110.1

Barton, N. H., & Gale, K. S. (1993). Genetic analysis of hybrid zones. In R. G. Harrison (Ed.), *Hybrid zones and the evolutionary process* (pp. 13–45). Oxford University Press. https://doi.org/10.1093/oso/9780195069174.001.0001

Barton, N. H., & Hewitt, G. M. (1985). Analysis of hybrid zones. *Annual Review of Ecology and Systematics*, *16*, 113–148. https://doi.org/10.1146/annurev.es.16.110185.000553

Blain, S. A., Justen, H. C., Langdon, Q. K., & Delmore, K. E. (2025). Repeatable selection on large ancestry blocks in an avian hybrid zone. *Molecular Biology and Evolution*, *42*(3), msaf044. https://doi.org/10.1093/molbev/msaf044

Brelsford, A., & Irwin, D. E. (2009). Incipient speciation despite little assortative mating: The yellow-rumped warbler hybrid zone. *Evolution*, *63*(12), 3050–3060. https://doi.org/10.1111/j.1558-5646.2009.00777.x

Brelsford, A., Toews, D. P. L., & Irwin, D. E. (2017). Admixture mapping in a hybrid zone reveals loci associated with avian feather coloration. *Proceedings of the Royal Society B: Biological Sciences*, *284*(1866), 20171106. https://doi.org/10.1098/rspb.2017.1106

Bryant, D., Bouckaert, R., Felsenstein, J., Rosenberg, N. A., & Roychoudhury, A. (2012). Inferring species trees directly from biallelic genetic markers: Bypassing gene trees in a full coalescent analysis. *Molecular Biology and Evolution*, *29*(8), 1917–1932. https://doi.org/10.1093/molbev/mss086

Campagna, L., Benites, P., Lougheed, S. C., Lijtmaer, D. A., Di Giacomo, A. S., Eaton, M. D., & Tubaro, P. L.. (2012). Rapid phenotypic evolution during incipient speciation in a continental avian radiation. *Proceedings of the Royal Society B: Biological Sciences*, *279*, 1847–1856. https://doi.org/10.1098/rspb.2011.2170

Campagna, L., Repenning, M., Silveira, L. F., Fontana, C. S., Tubaro, P. L., & Lovette, I. J. (2017). Repeated divergent selection on pigmentation genes in a rapid finch radiation. *Science Advances*, *3*(5), 1–11. https://doi.org/10.1126/sciadv.1602404

Capblancq, T., Després, L., & Mavárez, J. (2020). Genetic, morphological and ecological variation across a sharp hybrid zone between two alpine butterfly species. *Evolutionary Applications*, *13*(6), 1435–1450. https://doi.org/10.1111/eva.12925

Castaño, M. I., Croyle, E., Cadena, C. D., & Uy, J. A. C. (2026). Replicate avian hybrid zones reveal the progression of genetic and trait introgression through time. *Evolution*, *80*, 779–799.

Céspedes-Arias, L. N., Cuervo, A. M., Bonaccorso, E., Castro-Farias, M., Mendoza-Santacruz, A., Pérez-Emán, J. L., Witt, C. C., & Cadena, C. D. (2021). Extensive hybridization between two Andean warbler species with shallow divergence in mtDNA. *Ornithology*, *138*(1), 1–28. https://doi.org/10.1093/ornithology/ukaa065

Clements, J. F., Rasmussen, P. C., Schulenberg, T. S., Iliff, M. L., Gerbracht, J. A., Lepage, D., Spencer, A., Billerman, S. M., Sullivan, B. L., Smith, M., & Wood, C. L. (2025). *The eBird/Clements checklist of birds of the world: v2025*. https://www.birds.cornell.edu/clementschecklist/download/. Accessed March, 2026.

Cronemberger, Á. A., Aleixo, A., Mikkelsen, E. K., & Weir, J. T. (2020). Postzygotic isolation drives genomic speciation between highly cryptic Hypocnemis antbirds from Amazonia. *Evolution*, *74*(11), 2512–2525. https://doi.org/10.1111/evo.14103

Cuervo, A. M. (2013). *Evolutionary assembly of the neotropical montane avifauna*. Doctoral dissertation, Lousiana State University.

Cuervo, A. M., & Arias, L. N. C. (2023). The type of *Setophaga ruficoronata* (Kaup 1851) is a hybrid: Implications for the taxonomy of Myioborus warblers (Passeriformes: Parulidae). *Zootaxa*, *5383*(4), 476–490. https://doi.org/10.11646/zootaxa.5383.4.3

Curson, J., David, Q., & Beadle, D. (1994). *Warblers of the Americas: An identification guide*. Houghton Mifflin Harcourt.

Danecek, P., Auton, A., Abecasis, G., Albers, C. A., Banks, E., DePristo, M. A., Handsaker, R. E., Lunter, G., Marth, G. T., Sherry, S. T., McVean, G., & Durbin, R. (2011). The variant call format and VCFtools. *Bioinformatics*, *27*(15), 2156–2158. https://doi.org/10.1093/bioinformatics/btr330

de Zwaan, D. R., Mackenzie, J., Mikkelsen, E., Wood, C., & Wang, S. (2022). Pleiotropic opposing dominance within a color gene block contributes to a nascent species boundary via its influence on hybrid male territorial behavior. *PNAS Nexus*, *1*(3), pgac074. https://doi.org/10.1093/pnasnexus/pgac074

Del-Rio, G., Rego, M. A., Whitney, B. M., Schunck, F., Silveira, L. F., Faircloth, B. C., & Brumfield, R. T. (2022). Displaced clines in an avian hybrid zone (Thamnophilidae: Rhegmatorhina) within an Amazonian interfluve. *Evolution*, *76*(3), 455–475, https://doi.org/10.1111/evo.14377

DeRaad, D. A., Applewhite, E. E., Tsai, W. L. E., Terrill, R. S., Kingston, S. E., Braun, M. J., & McCormack, J. E. (2023). Hybrid zone or hybrid lineage: A genomic reevaluation of Sibley's classic species conundrum in Pipilo towhees. *Evolution*, *77*(3), 852–869. https://doi.org/10.1093/evolut/qpac068

Derryberry, E. P., Derryberry, G. E., Maley, J. M., & Brumfield, R. T. (2014). HZAR: Hybrid zone analysis using an R software package.

Molecular Ecology Resources, *14*(3), 652–663. https://doi.org/10.1111/1755-0998.12209

Dubay, S. G., & Witt, C. C. (2014). Differential high-altitude adaptation and restricted gene flow across a mid-elevation hybrid zone in Andean tit-tyrant flycatchers. *Molecular Ecology*, *23*(14), 3551–3565. https://doi.org/10.1111/mec.12836

Eaton, D. A. R., & Ree, R. H. (2013). Inferring phylogeny and introgression using RADseq data: An example from flowering plants (Pedicularis: Orobanchaceae). *Systematic Biology*, *62*(5), 689–706. https://doi.org/10.1093/sysbio/syt032

Edwards, S. V., Potter, S., Schmitt, C. J., Bragg, J. G., & Moritz, C. (2016). Reticulation, divergence, and the phylogeography-phylogenetics continuum. *Proceedings of the National Academy of Sciences*, *113*(29), 8025–8032. https://doi.org/10.1073/pnas.1601066113

Excoffier, L., Dupanloup, I., Huerta-Sánchez, E., Sousa, V. C., & Foll, M. (2013). Robust demographic inference from genomic and SNP data. *PLoS genetics*, *9*(10), e1003905. https://doi.org/10.1371/journal.pgen.1003905

Flantua, S. G., Hooghiemstra, H., Van Boxel, J. H., Cabrera, M., González-Carranza, Z., & González-Arango, C. (2014). Connectivity dynamics since the Last Glacial Maximum in the northern Andes; a pollen-driven framework to assess potential migration. In W. D. Stevens, O. M. Montiel, & P. H. Raven (Eds.), *Paleobotany and biogeography: A festschrift for Alan Graham in his 80th year* (pp. 98–123). Missouri Botanical Garden.

Friis, G., Aleixandre, P., Rodríguez-Estrella, R., Navarro-Sigüenza, A. G., & Milá, B. (2016). Rapid postglacial diversification and long-term stasis within the songbird genus Junco: Phylogeographic and phylogenomic evidence. *Molecular Ecology*, *25*(24), 6175–6195. https://doi.org/10.1111/mec.13911

Gay, L., Crochet, P. A., Bell, D. A., & Lenormand, T. (2008). Comparing clines on molecular and phenotypic traits in hybrid zones: A window on tension zone models. *Evolution*, *62*(11), 2789–2806. https://doi.org/10.1111/j.1558-5646.2008.00491.x

Gompert, Z., DeRaad, D. A., & Buerkle, C. A. (2024). A next generation of hierarchical Bayesian analyses of hybrid zones enables direct quantification of variation in introgression in R. *Ecology and Evolution*, *14*, 2003–2024. https://doi.org/10.1002/ece3.70548

Graham, C. H., Silva, N., & Velásquez-Tibatá, J. (2010). Evaluating the potential causes of range limits of birds of the Colombian Andes. *Journal of Biogeography*, *37*(10), 1863–1875. https://doi.org/10.1111/j.1365-2699.2010.02356.x

Graves, G. R. (1982). Speciation in the carbonated flower-piercer (*Diglossa carbonaria*) complex of the Andes. *The Condor*, *84*, 1–14. https://doi.org/10.2307/1367812

Graves, G. R. (1988). Linearity of geographic range and its possible effect on the population structure of Andean birds. *The Auk*, *105*(1), 47–52. https://doi.org/10.1093/auk/105.1.47

Gutiérrez-Pinto, N., Cuervo, A. M., Miranda, J., Pérez-Emán, J. L., Brumfield, R. T., & Cadena, C. D. (2012). Non-monophyly and deep genetic differentiation across low-elevation barriers in a Neotropical montane bird (*Basileuterus tristriatus*; Aves: Parulidae). *Molecular Phylogenetics and Evolution*, *64*(1), 156–165. https://doi.org/10.1016/j.ympev.2012.03.011

Harrison, R. G. (1986). Pattern and process in a narrow hybrid zone. *Heredity*, *56*(3), 337–349. https://doi.org/10.1038/hdy.1986.55

Harrison, R. G. (1990). Hybrid zones: Windows on evolutionary process. In D. Futuyma, & J. Antonovics (Eds.), *Oxford suurveys in evolutionary biology*. (Vol. 7, pp. 69–128). Oxford University Press.

Hazzi, N. A., Moreno, J. S., Ortiz-Movliav, C., & Palacio, R. D. (2018). Biogeographic regions and events of isolation and diversification of the endemic biota of the tropical Andes. *Proceedings of the National Academy of Sciences*, *115*(31), 7985–7990. https://doi.org/10.1073/pnas.1803908115

Irwin, D. E., Rubtsov, A. S., & Panov, E. N. (2009). Mitochondrial introgression and replacement between yellowhammers (*Emberiza citrinella*) and pine buntings (*Emberiza leucocephalos*) (Aves: Passeriformes). *Biological Journal of the Linnean Society*, *98*, 422–438. https://doi.org/10.1111/j.1095-8312.2009.01282.x

Kearns, A. M., Restani, M., Szabo, I., Schrøder-Nielsen, A., Kim, J. A., Richardson, H. M., Marzluff, J. M., Fleischer, R. C., Johnsen, A., & Omland, K. E. (2018). Genomic evidence of speciation reversal in ravens. *Nature Communications*, *9*(1), 906. https://doi.org/10.1038/s41467-018-03294-w

Kozlov, A. M., Darriba, D., Flouri, T., Morel, B., & Stamatakis, A. (2019). RAxML-NG: A fast, scalable and user-friendly tool for maximum likelihood phylogenetic inference. *Bioinformatics*, *35*(21), 4453–4455. https://doi.org/10.1093/bioinformatics/btz305

Leaché, A. D., & Oaks, J. R. (2017). The utility of single nucleotide polymorphism (SNP) data in phylogenetics. *Annual Review of Ecology, Evolution, and Systematics*, *48*, 69–84. https://doi.org/10.1146/annurev-ecolsys-110316-022645

Li, H., & Durbin, R. (2009). Fast and accurate short read alignment with Burrows–Wheeler transform. *Bioinformatics*, *25*(14), 1754–1760. https://doi.org/10.1093/bioinformatics/btp324

Lim, H. C., Bennett, K. F. P., Justyn, N. M., Powers, M. J., Long, K. M., Kingston, S. E., Lindsay, W. R., Pease, J. B., Fuxjager, M. J., Bolton, P. E., Balakrishnan, C. N., Day, L. B., Parsons, T. J., Brawn, J. D., Hill, G. E., & Braun, M. J. (2024). Sequential introgression of a carotenoid processing gene underlies sexual ornament diversity in a genus of manakins. *Science Advances*, *10*(47), eadn8339. https://doi.org/10.1126/sciadv.adn8339

Liu, S., Zhang, L., Sang, Y., Lai, Q., Zhang, X., Jia, C., Long, Z., Wu, J., Ma, T., Mao, K., Street, N. R., Ingvarsson, P. K., Liu, J., & Wang, J. (2022). Demographic history and natural selection shape patterns of deleterious mutation load and barriers to introgression across Populus genome. *Molecular Biology and Evolution*, *39*(2), 1–16. https://doi.org/10.1093/molbev/msac008

Long, K. M., Rivera-Colón, A. G., Bennett, K. F. P., Catchen, J. M., Braun, M. J., & Brawn, J. D. (2024). Ongoing introgression of a secondary sexual plumage trait in a stable avian hybrid zone. *Evolution*, *78*(9), 1539–1553. https://doi.org/10.1093/evolut/qpae076

Lopez, K. A., McDiarmid, C. S., Griffith, S. C., Lovette, I. J., & Hooper, D. M. (2021). Evaluating evidence of mitonuclear incompatibilities with the sex chromosomes in an avian hybrid zone. *Evolution*, *75*(6), 1395–1414. https://doi.org/10.1111/evo.14243

Lovette, I. J., Pérez-Emán, J. L., Sullivan, J. P., Banks, R. C., Fiorentino, I., Córdoba-Córdoba, S., Echeverry-Galvis, M., Barker, F. K., Burns, K. J., Klicka, J., Lanyon, S. M., & Bermingham, E. (2010). A comprehensive multilocus phylogeny for the wood-warblers and a revised classification of the Parulidae (Aves). *Molecular Phylogenetics and Evolution*, *57*(2), 753–770. https://doi.org/10.1016/j.ympev.2010.07.018

Malinsky, M., Trucchi, E., Lawson, D. J., & Falush, D. (2018). RADpainter and fineRADstructure: Population inference from RADseq data. *Molecular Biology and Evolution*, *35*(5), 1284–1290. https://doi.org/10.1093/molbev/msy023

Marchetti, K. (1992). Dark habitats and bright birds illustrate the role of the environment in species divergence. *Nature*, *362*, 149–152. https://doi.org/10.1038/362149a0

Marcus, J., Ha, W., Barber, R. F., & Novembre, J. (2021). Fast and flexible estimation of effective migration surfaces. *Elife*, *10*, 1–46. https://doi.org/10.7554/eLife.61927

Márquez, R., Linderoth, T. P., Mejía-Vargas, D., Nielsen, R., Amézquita, A., & Kronforst, M. R. (2020). Divergence, gene flow, and the origin of leapfrog geographic distributions: The history of colour pattern variation in *Phyllobates* poison-dart frogs. *Molecular Ecology*, *29*(19), 3702–3719. https://doi.org/10.1111/mec.15598

Martínez-Gómez, S. C., Lara, C. E., Remsen, J. V., Brumfield, R. T., & Cuervo, A. M. (2023). Unmasking hidden genetic, vocal, and size variation in the masked flowerpiercer along the Andes supports two species separated by Northern Peruvian Low. *Ornithology*, *140*(4), 1–14. https://doi.org/10.1093/ornithology/ukad028

Mayr, E. (1942). *Systematics and the origin of species from the viewpoint of a zoologist*. Columbia University Press.

Meirmans, P. G. (2012). The trouble with isolation by distance. *Molecular Ecology*, *21*(12), 2839–2846. https://doi.org/10.1111/j.1365-294X.2012.05578.x

Molloy, E. K., Durvasula, A., & Sankararaman, S. (2021). Advancing admixture graph estimation via maximum likelihood network orientation. *Bioinformatics*, *37*, i142–i150. https://doi.org/10.1093/bioinformatics/btab267

Morales-Rozo, A., Tenorio, E. A., Carling, M. D., & Cadena, C. D. (2017). Origin and cross-century dynamics of an avian hybrid zone. *BMC Evolutionary Biology*, *17*(1), 257. https://doi.org/10.1186/s12862-017-1096-7

Mullen, L. M., & Hoekstra, H. E. (2008). Natural selection along an environmental gradient: A classic cline in mouse pigmentation. *Evolution*, *62*, 1555–1570. https://doi.org/10.1111/j.1558-5646.2008.00425.x

Mumme, R. L. (2015). Demography of Slate-throated Redstarts (*Myioborus miniatus*): A non-migratory Neotropical warbler. *Journal of Field Ornithology*, *86*(2), 89–102. https://doi.org/10.1111/jofo.12093

Muñoz-Quintana, G., & Cuervo, A. (2024). Phenotypic variation and weak behavioral isolation in a putative hybrid zone between Andean Atlapetes brushfinches (Passerellidae). *BioRxiv*, https://doi.org/10.1101/2024.11.17.623919

Natola, L., Curtis, A., Hudon, J., & Burg, T. M. (2021). Introgression between *Sphyrapicus nuchalis* and *S. varius* sapsuckers in a hybrid zone in west-central Alberta. *Journal of Avian Biology*, *52*(8), 1–12. https://doi.org/10.1111/jav.02717

Nosil, P. (2008). Ernst Mayr and the integration of geographic and ecological factors in speciation. *Biological Journal of the Linnean Society*, *95*(1), 26–46. https://doi.org/10.1111/j.1095-8312.2008.01091.x

Nychka, D., Furrer, R., Paige, J., Sain, S., & Nychka, M. D. (2025). Package "fields". https://doi.org/10.5065/D6W957CT

Ocampo, D., Sandoval, L., & Uy, J. A. C. (2025). Weak premating reproductive isolation despite divergence in secondary sexual traits in the variable seedeater. *Animal Behaviour*, *221*, 123072. https://doi.org/10.1016/j.anbehav.2024.123072

Oksanen, J., Blanchet„ F. G., Friendly„ M., Kindt, R., Legendre, P., McGlinn„ D., Minchin„ P.R., O'Hara, B., Simpson„ G.L., Solymos„ P., Stevens, M. H. H., Szoecs„ E., & Wagner„ H. (2019). "The vegan package." Community ecology package. *R package. R package version, 25* (2018), https://cran.r-project.org/web/packages/vegan/index.html. Accessed July, 2023. Accessed July, 2023.

Paris, J. R., Stevens, J. R., & Catchen, J. M. (2017). Lost in parameter space: A road map for stacks. *Methods in Ecology and Evolution*, *8*(10), 1360–1373. https://doi.org/10.1111/2041-210X.12775

Pérez-Emán, J. L. (2005). Molecular phylogenetics and biogeography of the Neotropical redstarts (*Myioborus*; Aves, Parulinae). *Molecular Phylogenetics and Evolution*, *37*(2), 511–528. https://doi.org/10.1016/j.ympev.2005.04.013

Peterson, B. K., Weber, J. N., Kay, E. H., Fisher, H. S., & Hoekstra, H. E. (2012). Double digest RADseq: An inexpensive method for de novo SNP discovery and genotyping in model and non-model species. *PLoS ONE*, *7*(5), e37135. https://doi.org/10.1371/journal.pone.0037135

Pickrell, J. K., & Pritchard, J. K. (2012). Inference of population splits and mixtures from genome-wide allele frequency data. *PLoS Genetics*, *8*(11), e1002967. https://doi.org/10.1371/journal.pgen.1002967

Poelstra, J. W., Vijay, N., Bossu, C. M., Lantz, H., Ryll, B., Müller, I., Baglione, V., Unneberg, P., Wikelski, M., Grabherr, M. G., & Wolf, J. B. W. (2014). The genomic landscape underlying phenotypic integrity in the face of gene flow in crows. *Science*, *344*(6190), 1410–1414. https://doi.org/10.1126/science.1253226

Pool, J. E., & Nielsen, R. (2009). Inference of historical changes in migration rate from the lengths of migrant tracts. *Genetics*, *181*(2), 711–719. https://doi.org/10.1534/genetics.108.098095 .

Pozo-Zamora, G. M., Krabbe, N., Mena-Valenzuela, P., Nilsson, J., & Brito, J. (2022). Birds of the Cordillera del Kutukú, Morona Santiago, Southeastern Ecuador. *Revista Peruana de Biología*, *29*(1), e20667. https://doi.org/10.15381/RPB.V29I1.20667

Price, T. (2008). *Speciation in birds*. Robert and Co.

Prieto-Torres, D. A., Cuervo, A. M., & Bonaccorso, E. (2018). On geographic barriers and Pleistocene glaciations: Tracing the diversification of the Russet-crowned Warbler (*Myiothlypis coronata*) along the Andes. *PLoS ONE*, *13*(3), e0191598. https://doi.org/10.1371/journal.pone.0191598

Pulido-Santacruz, P., Aleixo, A., & Weir, J. T. (2018). Morphologically cryptic amazonian bird species pairs exhibit strong postzygotic reproductive isolation. *Proceedings of the Royal Society B: Biological Sciences*, *285*(1874),

Rahbek, C., Borregaard, M. K., Colwell, R. K., Dalsgaard, B., Holt, B. G., Morueta-Holme, N., Nogues-Bravo, D., Whittaker, R. J., & Fjeldså, J. (2019). Humboldt's enigma: What causes global patterns of mountain biodiversity? *Science*, *365*(6458), 1108–1113. https://doi.org/10.1126/science.aax0149

Ramírez-Barahona, S., & Eguiarte, L. E. (2013). The role of glacial cycles in promoting genetic diversity in the Neotropics: The case of cloud forests during the Last Glacial Maximum. *Ecology and Evolution*, *3*(3), 725–738. https://doi.org/10.1002/ece3.483

Remsen, J. V. (1984). High incidence of "Leapfrog" pattern of geographic variation in Andean birds: Implications for the speciation process. *Science*, *224*, 171–173. https://doi.org/10.1126/science.224.4645.171

Remsen, J. V., Cadena, C. D., Jaramillo, A., Nores, M., Pacheco, J. F., Robbins, M. B., Schulenberg, T. S., Stiles, F. G., Stotz, D. F., & Zimmer, K. J. (2026). *A classification of the bird species of South America*. American Ornithological Society. http://www.museum.lsu.edu/~Remsen/SACC.html

Rémy, A., Grégoire, A., Perret, P., & Doutrelant, C. (2010). Mediating male-male interactions: The role of the UV blue crest coloration in blue tits. *Behavioral Ecology and Sociobiology*, *64*(11), 1839–1847. https://doi.org/10.1007/s00265-010-0995-z

Rivera-Colón, A. G., & Catchen, J. (2022). Population genomics analysis with RAD, Reprised: Stacks 2 (Chapter 7). In C. Verde, & D. Giordano (Eds.), *Marine genomics: Methods and protocols*. Springer Nature-Humana Press.

Robbins, M. B., Ridgely, R. S., & Schulenberg, T. S. (1987). The avifauna of the Cordillera de Cutucut, Ecuador, with Comparisons to other Andean Localities. *Proceedings of The Academy of Natural Sciences of Philadelphia*, *139*(1), 243–259.

Rochette, N. C., Rivera-Colón, A. G., & Catchen, J. M. (2019). Stacks 2: Analytical methods for paired-end sequencing improve RADseq-based population genomics. *Molecular Ecology*, *28*(21), 4737–4754. https://doi.org/10.1111/mec.15253

Rubin, B. E. R., Ree, R. H., & Moreau, C. S. (2012). Inferring phylogenies from RAD sequence data. *PLoS ONE*, *7*(4), 1–12. https://doi.org/10.1371/journal.pone.0033394

Sambrook, J. (1987). *Molecular cloning: A laboratory manual*. Cold Spring Harbor Laboratory.

Sanín, M. J., Cardona, A., Céspedes Arias, L. N., González-Arango, C., Pardo, N., & Cadena, C. D. (2024). Volcanoes, evolving landscapes, and biodiversity in Neotropical mountains. *Frontiers of Biogeography*, *16*(1), 1–14. https://doi.org/10.21425/F5FBG61882

Schmitt, C. J. (2022). *Phylogeography, color variation, and hybridization in an andean tanager, superciliaried hemispingus (Aves: Thlypopsis superciliaris). [Doctoral dissertation]*. Harvard University.

Scordato, E. S. C., Wilkins, M. R., Semenov, G., Rubtsov, A. S., Kane, N. C., & Safran, R. J. (2017). Genomic variation across two barn swallow hybrid zones reveals traits associated with divergence in sympatry and allopatry. *Molecular Ecology*, *26*(20), 5676–5691. https://doi.org/10.1111/mec.14276

Scott, G. W., & Deag, J. M. (1998). Blue tit (*Parus caeruleus*) agonistic displays: A reappraisal. *Behaviour*, *135*(6), 665–691. https://doi.org/10.1163/156853998792640431

Seeholzer, G. F., & Brumfield, R. T. (2018). Isolation by distance, not incipient ecological speciation, explains genetic differentiation in an Andean songbird (Aves: Furnariidae: *Cranioleuca antisiensis*, Line-cheeked Spinetail) despite near threefold body size change across an

environmental gradien. *Molecular Ecology*, *27*(1), 279–296. https://doi.org/10.1111/mec.14429

Semenov, G. A., Linck, E., Enbody, E. D., Harris, R. B., Khaydarov, D. R., Alström, P., Andersson, L., & Taylor, S. A. (2021). Asymmetric introgression reveals the genetic architecture of a plumage trait. *Nature Communications*, *12*(1), 1–9. https://doi.org/10.1038/s41467-021-21340-y

Sonne, J., Dalsgaard, B., Borregaard, M. K., Kennedy, J., Fjeldså, J., & Rahbek, C. (2022). Biodiversity cradles and museums segregating within hotspots of endemism. *Proceedings of the Royal Society B: Biological Sciences*, *289*(1981),. https://doi.org/10.1098/rspb.2022.1102

Stein, A. C., & Uy, J. A. C. (2006a). Plumage brightness predicts male mating success in the lekking golden-collared manakin, *Manacus vitellinus*. *Behavioral Ecology*, *17*(1), 41–47. https://doi.org/10.1093/beheco/ari095

Stein, A. C., & Uy, J. A. C. (2006b). Unidirectional introgression of a sexually selected trait across an avian hybrid zone: A role for fehoice? *Evolution*, *60*(7), 1476–1485. https://doi.org/10.1111/j.0014-3820.2006.tb01226.x

Stoltz, M., Baeumer, B., Bouckaert, R., Fox, C., Hiscott, G., & Bryant, D. (2021). Bayesian inference of species trees using diffusion models. *Systematic Biology*, *70*(1), 145–161. https://doi.org/10.1093/sysbio/syaa051

Stryjewski, K. F., & Sorenson, M. D. (2017). Mosaic genome evolution in a recent and rapid avian radiation. *Nature Ecology & Evolution*, *1*(12), 1912–1922. https://doi.org/10.1038/s41559-017-0364-7

Taylor, S. A., Curry, R. L., White, T. A., Ferretti, V., & Lovette, I. (2014). Spatiotemporally consistent genomic signatures of reproductive isolation in a moving hybrid zone. *Evolution*, *68*(11), 3066–3081. https://doi.org/10.1111/evo.12510

Thrasher, D. J., Butcher, B. G., Campagna, L., Webster, M. S., & Lovette, I. J. (2018). Double-digest RAD sequencing outperforms microsatellite loci at assigning paternity and estimating relatedness: A proof of concept in a highly promiscuous bird. *Molecular Ecology Resources*, *18*(5), 953–965. https://doi.org/10.1111/1755-0998.12771

Toews, D. P. L., & Brelsford, A. (2012). The biogeography of mitochondrial and nuclear discordance in animals. *Molecular Ecology*, *21*, 3907–3930. https://doi.org/10.1111/j.1365-294X.2012.05664.x

Toews, D. P. L., Campagna, L., Taylor, S. A., Balakrishnan, C. N., Baldassarre, D. T., Deane-Coe, P. E., Harvey, M. G., Hooper, D. M., Irwin, D. E., Judy, C. D., Mason, N. A., McCormack, J. E., McCracken, K. G., Oliveros, C. H., Safran, R. J., Scordato, E. S. C., Stryjewski, K. F., Tigano, A., Uy, J. A. C., … Winger, B. M. (2016a). Genomic approaches to understanding the early stages of population divergence and speciation in birds. *The Auk*, *133*, 13–30. https://doi.org/10.1642/AUK-15-51.1

Toews, D. P. L., Taylor, S. A., Vallender, R., Brelsford, A., Butcher, B., Messer, P. W., & Lovette, I. J. (2016b). Plumage genes and little else distinguish the genomes of hybridizing warblers. *Current Biology*, *26*(17), 2313–2318. https://doi.org/10.1016/j.cub.2016.06.034

Uy, J. A. C., Irwin, D. E., & Webster, M. S. (2018). Behavioral isolation and incipient speciation in birds. *Annual Review of Ecology, Evolution, and Systematics*, *49*, 1–24. https://doi.org/10.1146/annurev-ecolsys-110617-062646

Uy, J. A. C., Moyle, R. G., & Filardi, C. E. (2009). Plumage and song differences mediate species recognition between incipient flycatcher species of the Solomon Islands. *Evolution*, *63*(1), 153–164. https://doi.org/10.1111/j.1558-5646.2008.00530.x

Vos, M., & Velicer, G. J. (2008). Isolation by distance in the spore-forming soil bacterium *Myxococcus xanthus*. *Current Biology*, *18*(5), 386–391. https://doi.org/10.1016/j.cub.2008.02.050

Vuilleumier, F. (1969). Pleistocene speciation of birds living in the high Andes. *Nature*, *223*, 1179–1180. https://doi.org/10.1038/2231179a0

Wagner, C. E., Keller, I., Wittwer, S., Selz, O. M., Mwaiko, S., Greuter, L., Sivasundar, A., & Seehausen, O. (2013). Genome-wide RAD sequence data provide unprecedented resolution of species boundaries and relationships in the Lake Victoria cichlid adaptive radiation. *Molecular Ecology*, *22*(3), 787–798. https://doi.org/10.1111/mec.12023

Weir, B. S., & Cockerham, C. C. (1984). Estimating F-statistics for the analysis of population structure. *Evolution*, *38*(6), 1358–1370. https://doi.org/10.1111/j.1558-5646.1984.tb05657.x

Weir, J. T., Faccio, M. S., Pulido-Santacruz, P., Barrera-Guzmán, A. O., & Aleixo, A. (2015). Hybridization in headwater regions, and the role of rivers as drivers of speciation in Amazonian birds. *Evolution*, *69*(7), 1823–1834. https://doi.org/10.1111/evo.12696

Wiens, B. J., DeCicco, L. H., & Colella, J. P. (2025). triangulaR: An R package for identifying AIMs and building triangle plots using SNP data from hybrid zones. *Heredity*, *134*, 251–262. https://doi.org/10.1038/s41437-025-00760-2

Winger, B. M. (2017). Consequences of divergence and introgression for speciation in Andean cloud forest birds. *Evolution*, *71*(7), 1815–1831. https://doi.org/10.1111/evo.13251

Winger, B. M., & Bates, J. M. (2015). The tempo of trait divergence in geographic isolation: Avian speciation across the Marañon Valley of Peru. *Evolution*, *69*(3), 772–787. https://doi.org/10.1111/evo.12607

Yi, X., & Latch, E. K. (2022). Nonrandom missing data can bias principal component analysis inference of population genetic structure. *Molecular Ecology Resources*, *22*(2), 602–611. https://doi.org/10.1111/1755-0998.13498

Zamudio, K. R., Bell, R. C., & Mason, N. A. (2016). Phenotypes in phylogeography: Species' traits, environmental variation, and vertebrate diversification. *Proceedings of the National Academy of Sciences*, *113*(29), 8041–8048. https://doi.org/10.1073/pnas.1602237113

Zheng, X. (2013). *SNPRelate: A high-performance computing toolset for relatedness and principal component analysis of SNP data*. (R package version 0.9.19). http://core.bioconductor.org/packages/release/bioc/html/SNPRelate.html Accessed July, 2019.

Zimmer, J. T. (1949). Studies of Peruvian birds. No. 54, The families Catamblyrhynchidae and Parulidae. *American Museum Novitates*, *1428*, 1–59.

Received August 25, 2025; revisions received March 27, 2026; accepted April 24, 2026
Associate Editor: Scott Taylor; Handling Editor: Hélène Morlon